catalysts

MDPI

Review

Determinants for an Efficient Enzymatic Catalysis in Poly(Ethylene Terephthalate) Degradation

José Augusto Castro-Rodríguez [1], Rogelio Rodríguez-Sotres [2] and Amelia Farrés [1,*]

[1] Departamento de Alimentos y Biotecnología, Facultad de Química, Universidad Nacional Autónoma de México, Mexico City 04510, Mexico
[2] Departamento de Bioquímica, Facultad de Química, Universidad Nacional Autónoma de México, Mexico City 04510, Mexico
* Correspondence: farres@unam.mx

Abstract: The enzymatic degradation of the recalcitrant poly(ethylene terephthalate) (PET) has been an important biotechnological goal. The present review focuses on the state of the art in enzymatic degradation of PET, and the challenges ahead. This review covers (i) enzymes acting on PET, (ii) protein improvements through selection or engineering, (iii) strategies to improve biocatalyst–polymer interaction and monomer yields. Finally, this review discusses critical points on PET degradation, and their related experimental aspects, that include the control of physicochemical parameters. The search for, and engineering of, PET hydrolases, have been widely studied to achieve this, and several examples are discussed here. Many enzymes, from various microbial sources, have been studied and engineered, but recently true PET hydrolases (PETases), active at moderate temperatures, were reported. For a circular economy process, terephtalic acid (TPA) production is critical. Some thermophilic cutinases and engineered PETases have been reported to release terephthalic acid in significant amounts. Some bottlenecks in enzyme performance are discussed, including enzyme activity, thermal stability, substrate accessibility, PET microstructures, high crystallinity, molecular mass, mass transfer, and efficient conversion into reusable fragments.

Keywords: PET hydrolases; mass transfer; catalytic efficiency; enzyme kinetics; chimeras; adsorption; high crystallinity; PET microstructures

check for updates

Citation: Castro-Rodríguez, J.A.; Rodríguez-Sotres, R.; Farrés, A. Determinants for an Efficient Enzymatic Catalysis in Poly(Ethylene Terephthalate) Degradation. *Catalysts* **2023**, *13*, 591. https://doi.org/10.3390/catal13030591

Academic Editors: Rosa María Oliart-Ros and María Guadalupe Sánchez-Otero

Received: 10 February 2023
Revised: 6 March 2023
Accepted: 12 March 2023
Published: 15 March 2023

Copyright: © 2023 by the authors. Licensee MDPI, Basel, Switzerland. This article is an open access article distributed under the terms and conditions of the Creative Commons Attribution (CC BY) license (https://creativecommons.org/licenses/by/4.0/).

1. Introduction

The worldwide production of synthetic oil-based plastics has increased steadily, reaching around 390 million tons in 2021. The main industrial plastics are poly(propylene), low- and high-density poly(ethylene), poly(vinyl chloride), poly(ethylene terephthalate) (PET), poly(urethane), and poly(styrene) [1]. All these plastics are pollutants, affect ecosystems globally, and are resistant to biological degradation. Plastic pollutants can be found in the air [2], water bodies [3], salt [4], in several elements of the food chain [5], and can internalize in some cells [6]. Plastic pollution poses a serious environmental and health threat [7].

PET is a thermoplastic polyester composed of ethylene glycol (EG) and terephthalic acid (TPA), linked via ester bonds [8]. PET contains both amorphous and crystalline microstructures. The amorphous region has a flexible amorphous fraction (X_{MAF}) and a rigid amorphous fraction (X_{RAF}). EG in X_{MAF} is mainly in the *gauche* conformation, and a minor proportion is in the *trans* conformation. The X_{RAF} forms an interface between the crystalline regions (X_C), where the *trans*-conformation is predominant [9,10]. At the glass transition temperature (Tg) or above, the crystalline glassy state converts into an amorphous "soft and rubbery" state [11]. The Tg value of a PET sample depends on the starting nature of the polymer, as well as treatment conditions. The reported Tg value is around 65 °C for amorphous PET, 70–81 °C for semi-crystalline PET in air, and 60–65 °C in water [12,13]. The Tg depends not only on the polymer's initial crystallinity, but also

on its previous thermal history [14] and age [15]. Properties like crystallinity, molecular weight, surface area and charge, shape, size, microstructures, physicochemical properties of substrates, and the presence of additives, are significant to PET recycling, because these limit the polymer's biodegradability [16].

Beverage bottles, food packing containers, fibers, and films can be derived from PET resins [12]. Many PET products are single-use and contribute significantly to the daily urban plastic waste. Every consumer can change the final destiny of his/her waste materials. Unfortunately, a significant amount of residual PET goes to municipal solid waste landfills and into natural water bodies, mainly the oceans [3].

Nowadays, there are some alternatives for PET waste management:

(i) Mechanical recycling, which has limitations due to the loss of PET's properties.
(ii) Chemical degradation, which uses and produces compounds harmful to the environment. The specifics of these technologies have been reviewed elsewhere [17,18]. Briefly, some available chemical treatments are: hydrolysis (acidic, neutral, or basic) at high temperature and pressure, to render TPA; glycolysis at 180–240 °C under an inert atmosphere, to produce BHET; aminolysis at 20–200 °C, to yield terephthalic acid diamides plus oligomeric diacids; ammonolysis, consisting in PET treatment with zinc acetate at 70–180 °C under high pressure, to generate terephthalamide; and methanolysis, using methanol at 180–280 °C, and under 20 to 40 atm, to release EG and dimethyl terephthalate (DMT). Nevertheless, the need for product purification, their poor selectivity, and the possible contamination of catalysts by the presence of other plastics, impact the cost of these forms of recycling.
(iii) PET incineration, which generates energy, but has the drawback of CO_2 emission, and may release some toxic fumes [19].
(iv) Recycling by biotechnological degradation (Figure 1).

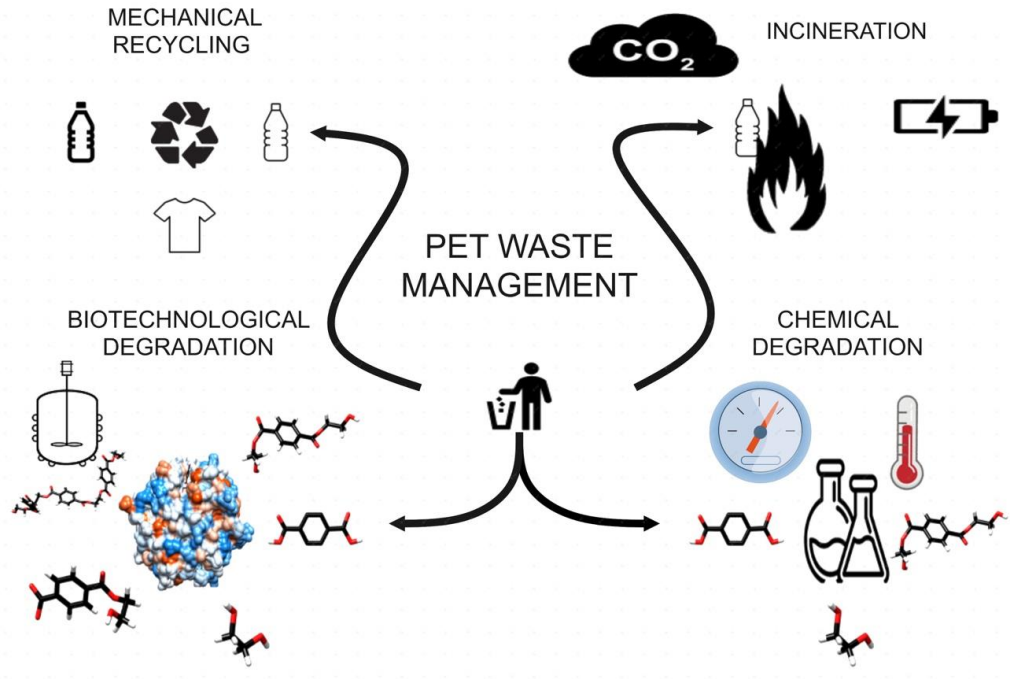


Figure 1. Treatments for PET waste management.

Of the above alternatives, recycling may produce different oligomers (bis (2-hydroxyethyl) terephthalate (BHET), mono (2-hydroxyethyl) terephthalate (MHET), DMT, and monomers (EG and TPA), and only these last are genuinely eco-friendly. Efficient recovery of monomers is central to proper recycling, as the newly synthesized PET resin will make bottles, containers, and fibers of uniform quality over and over, an actual circular economy. Furthermore,

TPA is a raw material in value-added products, like metal-organic frameworks for antibiotic-contaminated wastewater remediation, and other applications [20]. TPA can also be used as a raw material to produce bio-hydrogen, bioethanol, bio-methane, and biodiesel by microalgae [21]. All these products may be useful. Large oligomers could be used as a carbon source for *Taonella mepensis,* to enhance the yield and productivity of bacterial cellulose [22], or can be incorporated into bricks, paints, or roof coating formulations.

PET is a non-biodegradable recalcitrant semi-crystalline polyester. Nevertheless, in the last two decades, an intensive search for enzymes or microorganisms able to split long PET molecules into smaller chains, and ideally into monomers, has unveiled some promising candidates. Examples of microorganisms able to biodegrade PET are: *Microsphaerosis arundis* [23], *Ideonella sakaiensis* 201-F6 [24], *Camamonas testoterones* F6 [25], *Bacillus subtilis* [26], *Aspergillus niger* [26], *Spirulina sp.* [27], *Bacillus cereus* [28], *Stenotrophomonas pavanii* [29], *Bacillus pseudomycoides* [30], and some species from *Streptomyces* [31]. However, PET biodegradation by wild-type microorganisms takes months, even for small samples, thus, these might be used in landfill strategies where time is less important, and energy is not spent on the control of cultivation conditions. Additionally, there are some engineered microbes, which have been designed to break PET into monomers and use them as a carbon source, to support the biosynthesis of valuable chemicals [32]. Nonetheless, the use of genetically modified organisms must follow tight security guidelines. For instance, a mesophilic engineered *Pseudomonas putida* was able to depolymerize PET, and grow with TPA and EG as a carbon source; but the PET hydrolase genes had expression problems and only genomic integration with thermo-induction was successful. The recombinant bacteria were able to hydrolyze only 1.5% of the PET, after 6 days, at 37 °C. In addition, some engineered microbes were used to display PET hydrolases on their cell surface, however, these only generated less than 1 mM of mixed products [33–35]. A case with better success, was the thermophilic engineered *Clostridium thermocellum,* expressing a PET hydrolase. When cultured at 60 °C (170 rpm), close to the Tg, the digested PET lost 60% weight in 14 days, releasing TPA and MHET [36]. These examples show that the efficiency of PET degradation depends on the catalytic activity of the enzymes expressed, and cultivation conditions. Consequently, PET biodegradation by whole microorganisms lacks enough efficiency, as their attack mainly cleaves fibers at the polymer's surface, and the complete degradation is relatively slow. Restricted access to the inner polymer fibers contributes to PET's biodegradation recalcitrance. It is therefore necessary to design enzymes, chimeras, or enzyme mixtures with high activity against any type of PET sample. The appropriate choice of conditions for the enzymatic degradation of PET, is also essential. Factors such as the enzyme source, PET pretreatment, reaction temperature, mass transfer, enzyme to substrate ratio, additives, pH, and reaction medium, are all amenable variables to EG and TA yield optimization.

2. Enzymes Acting on PET

Since PET is a solid, and its constituents are hydrophobic, the fibers' degradation must take place at the solid–liquid interphase. According to Kawai et al. [37], two types of enzymes are currently known to act on PET. The first one consists of enzymes attacking the polymer surface, thus increasing its surface hydrophilicity, with little or no effect on the polymer morphology. Enzymes such as unspecific esterases, lipases, cutinases, serine proteases, and some true PETases may belong to this group. A second type is true PET hydrolases, which usually derive from thermostable cutinases, thermostable enzymes from compost metagenome libraries, and true PETase variants. These enzymes break the inner blocks of PET and change its structure, and some of them are potentially useful for bio-recycling. These enzymes have an open and shallow active site, lack any kind of lid domain, present moderate to high thermostability, show high affinity for the PET surface, and possess high specificity towards the PET ester bonds. This last group is the type of enzymes under focus in this review.

The Enzyme Commission classifies cutinase (EC 3.1.1.74) as a carboxylic ester hydrolase with an α/β fold. These enzymes possess the catalytic triad Ser–His–Asp, with a pre-existing oxyanion hole. Cutinases share some enzymatic and molecular properties with lipases, esterases, serine-proteases, and true PETases. Many of the best-characterized cutinases belong to actinomycetes or fungi, and these enzymes can cleave both small-molecule esters and polyesters resembling its complex natural substrate, cutin [38,39]. Another kind of enzyme is *Is*PETase, from *Ideonella sakaiensis* (EC. 3.1.1.101), which is a homolog of actinomycetal cutinases (46–52% amino acid identity) [13], but in nature, more enzymes are likely to be active against PET, and might be found in the future, i.e., the search should continue, as an example, BhrPETase, from the bacterium HR29 [40]. Given their similarity, it is worth asking what the differences between native cutinases and the native *Is*PETase are? Both share the fold, the catalytic triad Ser–His–Asp, a hydrophobic and flexible, yet solvent-exposed, substrate-binding cleft. However, this hydrophobic cleft is wider in *Is*PETase than in cutinases [41]. This is caused by a longer β8–α6 loop in *Is*PETase [42]. In addition, *Is*PETase has a more polarized surface charge, and it features two disulfide bonds, in contrast to only one found in actinomycetal cutinases [43]. Instead, cutinases are more thermostable, and some may contain ion-binding sites, which increase their melting temperature (Tm) and improve their catalytic activity. *Is*PETase's amino acid residues, S214, S238 [9], and I218 are essential for its activity, because they give more freedom to W185, an active-site neighboring residue [44]. Single and double mutants have confirmed the role of these residues in this and other enzyme orthologs. Thus, in *Is*PETase, W185 takes a crucial role, since it can adopt three conformations to accommodate the PET substrate (Figure 2) [9].

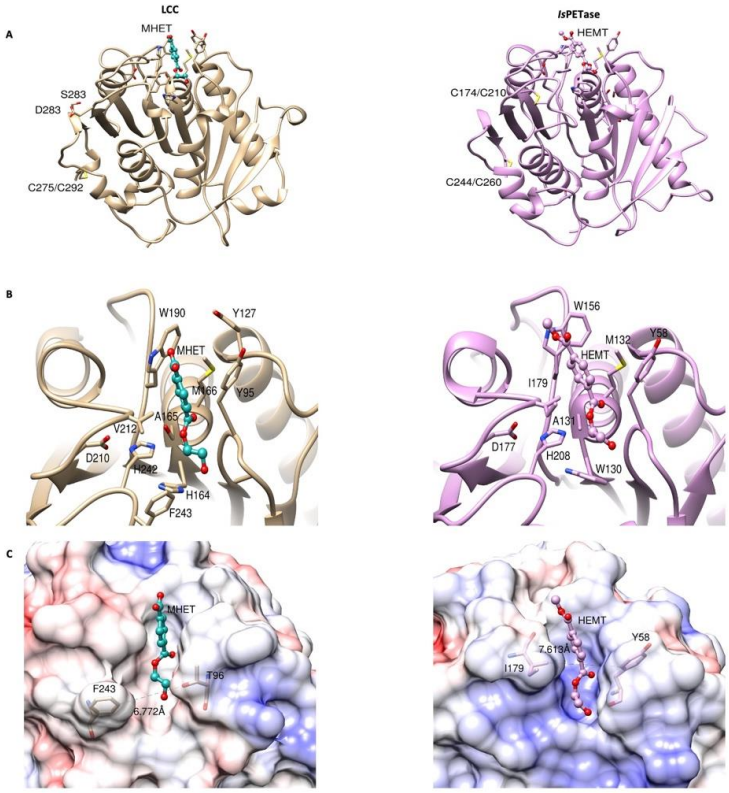


Figure 2. Complex structures of PET hydrolases with MHET and 1-(2-hydroxyethyl) 4-methyl terephthalate (HEMT). (**A**) Model representations of LCC/MHET (**left**) and *Is*PETase-S131A/HEMT (**right**). Two disulfide bridges are shown in *Is*PETase and one disulfide bridge in LCC. (**B**) View of the enzyme-substrate interaction network for both enzymes and catalytic residues. (**C**) Substrate-binding cleft of LCC and *Is*PETase, shown with coulombic electrostatic surface (blue is a positive charge and red is a negative charge). The dashes indicate the width of the substrate-binding cleft.

To obtain efficient PET bio-recycling tools, currently, the best enzyme candidates for improvement, by means of protein engineering, seem to be the thermostable cutinases from *Thermobifida fusca* [45], *Humicola insolens* [46], *Sacchamonosporas viridis* [47], LC-cutinase (LCC) [48], PHL7 or PES-H1 [49,50], BhrPETase [40], and some *Is*PETase variants [51]. Other possible candidates worth mentioning, are the enzymes from *Thermobifida cellulosilytica* [52–54].

3. Important Aspects Related to the Use of These Enzymes in Degradation and Bio-Recycling of PET

A natural selective pressure for a true PETase was not present before the introduction of *Dacron*™ by DuPont, in the 1940s. Since the introduction of the PET bottle in 1973 [55], this polymer became a significant environmental pollutant and constituted a new niche available for novel microorganisms to evolve. The first evidence of polyester biodegradation was reported only 20 years later [56]. Nevertheless, significant progress has been made, and some selected advances are summarized here.

A potential PET hydrolase was found in *Thermobifida fusca*. This wild-type enzyme hydrolyzed PET films. Müller et al. [45] observed a 50% weight loss after three weeks of treatment, but found no evidence of TPA accumulation. Furthermore, they analyzed the effect of this enzymatic activity on PET crystallinity and glass transition temperature, and tested the enzyme on samples of several PET types.

By contrast, Herrero Acero et al. [52] reported two wild-type cutinases (Thc_Cut1 and Thc_Cut2), cloned in *Escherichia coli,* from *Thermobifida cellulosilytica* DSM44535. Thc_Cut1 hydrolyzed PET films (37% crystallinity), releasing TPA and MHET products, while Thc_Cut2 generated more MHET than TPA. These differences contrast with their 93% of sequence identity and their nearly identical active site three-dimensional structures, as predicted from homology modeling. However, the electrostatic potential and hydrophobicity on their surfaces differ in two regions near the active site, a possible explanation for the differences in specificity [57].

A wild-type putative cutinase gene (Cut190) was cloned from *Saccharomonospora viridis,* in *E. coli*. The wild-type Cut190 hydrolyzed PET film and released TPA traces, when it was incubated overnight at 50 °C [47].

The already mentioned *Is*PETase (Figure 2, right panels), could release a small amount of TPA, and mostly MHET, from a PET film, but for a high-crystallinity PET sample, the enzyme released very little TPA and a small amount of MHET [24].

The gene encoding a cutinase homolog, LCC, was cloned from a library of a leaf-branch compost meta-genome, in *E. coli*. The purified recombinant LCC (Figure 2, left panels) showed hydrolytic activity against PET, at 50 °C, with gentle shaking [48].

Araújo et al. [58] reported a moderate TPA release from commercial polyester taffeta fabric, using the fungal cutinase from *Fusarium solani*.

Another attractive fungal cutinase (HiC) from *Thermomyces insolens* (formerly *Humicola insolens*), was able to degrade 97% of a PET film at 70 °C. These authors also reported the effects of buffer concentration, temperature, and PET nature, on the TPA yield [46].

Additionally, Sonnendecker et al. [49] cloned and expressed, in *E. coli,* the recombinant PHL7, which features an essential residue, L210, proposed to contribute to the binding of PET substrate, and considered to be responsible for its high activity. By contrast, other PET hydrolases have phenylalanine at the equivalent position. As with *Is*PETase, the active site pocket of PHL7 is larger than that of LCC, and accordingly, this enzyme also showed a high initial rate of hydrolysis and caused a substantial weight loss to amorphous PET films from Goodfellow Ltd. (GF-PET), at reaction temperatures up to 80 °C. Then, at longer incubation times, the TPA:MHET ratio increased, as PHL7 depolymerized up to 90% of PET films after 16 h, using 0.6 mg_{enzyme} $g_{PET}{}^{-1}$, at 70 °C. The enzyme's specific activity was high (91 mg_{TPAeq} h^{-1} $mg_{enzyme}{}^{-1}$), but PHL7 could not degrade biaxially oriented PET of higher crystallinity.

Many of the reports mentioned in the preceding paragraphs have a common finding: some of these enzymes can release TPA but only with low efficiency, and the basis of such low efficiency is not yet completely clear. Therefore, there are unresolved questions:

(i) Does catalytic efficiency limit PET hydrolysis by these enzymes?
(ii) Are the interfacial diffusion rate and the affinity for the PET surface critical steps in the degradation process?
(iii) Are the reaction conditions required for optimal TPA production yet to be found?

From these considerations, many parameters stand out as variables amenable to optimization. Variables such as temperature, pH, buffer concentration, crystallinity, molecular mass, and PET structure need detailed exploration for each of the promising candidate enzymes mentioned above. While many reports have optimized one or more of these factors, further improvements are still possible. Unfortunately, these are unlikely to be spectacular for native enzymes, and protein engineering will probably take a central role in the solution to the problem.

3.1. Protein Improvements through Selection or Engineering

As already mentioned, hydrolysis of PET is a heterogeneous and complex enzyme reaction, involving a liquid phase with a colloid and a partially solvated solid phase. The enzyme acts with a hip-hop mechanism, and the first step is the adsorption of the enzyme onto the PET surface, followed by ester bond cleavage and enzyme desorption, to start a new cycle [59–62]. Many strategies have been evaluated so far to improve PET degradation, to increase the recovery of TPA. We discuss these advancements here.

One, focuses on improving the enzymatic specificity constant (k_{cat}/K_M) toward PET, but the kinetic analysis must consider the surface concentration and adsorption constant [63,64]. Unfortunately, not all reports consider the complexities of the kinetic model and choose a more simplistic analysis, using the Michaelis-Menten classic kinetics (see, for instance, [52]).

A second research target is the thermal stability of the enzymes because, ideally, the protein should not unfold below the PET's Tg, and the enzyme should be highly active at about this temperature. Attempts to enhance the enzyme–PET interaction should not make the interaction too stable, because then the enzyme may remain attached to the polymer after completing the hydrolytic cycle, thus slowing down the product release step and making it rate-limiting [65].

The third research target is BHET and MHET hydrolysis. These act as competitive inhibitors in the reaction, and enzymes' hydrolysis rates may sometimes become too slow. However, inhibition was not detected for enzymes such as HiC and Cut190 [54,66–71].

3.1.1. Enzyme Kinetics

Enzyme kinetics requires an understanding of the enzyme and its relationship with a heterogeneous substrate, which complicates the conventional enzyme kinetics model of Michaelis-Menten (MM). Bååth et al. [60] applied a steady-state approximation for solid substrates, called the inverse MM framework. For MM, saturation reflects the substrate's nearly complete occupation of active sites. For inverse MM, saturation of target sites may occur, at high enzyme concentration, as attack sites (Γ_{attack}) on the polymer surface become occupied. However, this approximation has limitations, since it only applies to the situation when the reaction progress is at a low degree of substrate conversion, mainly at the beginning of the reaction, when there is a clear correlation between the number of ester bonds and the accessible surface of the PET [72]. These authors determined the kinetic parameters for three PET hydrolases (HiC, TfC, and *Is*PETase). The k_{cat} values reported were between 0.02 and 0.7 s^{-1}, close to carboxyl esterases' k_{cat} values for soluble substrates (3–30 s^{-1}). In this comparison, the turnover rate of the enzyme acting on intact PET depends on interactions with the polymeric substrate, but the chemical steps associated with the hydrolytic reaction should happen at similar rates. In the affinities case, $^{molar}K_M$ values were between 4 and 102 nM for HiC and TfC, values that indicate a very strong

substrate–enzyme interaction. The K_M for most wild-type enzymes, acting on naturally occurring substrates soluble in the bulk phase, is between 0.01 to 1 mM.

For the inverse MM model, the specificity constant was defined as the ratio of k_{cat} to $K_{M,}$ considering the total number of cleavable sites, Γ_{attack}, and this value, designated as $^{molar}\eta$, was in the range 10^5 to 10^7 $M^{-1}s^{-1}$ for solid PET, and 10^2 to 10^5 $M^{-1}s^{-1}$, for soluble PET oligomers. With soluble oligomers, the bigger the fragment, the higher the specificity constant, reaching a plateau for insoluble PET [73]. This $^{molar}\eta$ value, is comparable to other natural substrate–enzyme systems, such as microcrystalline cellulose and cellulases. HiC had the highest $^{molar}\eta$, apparently because of its better non-specific absorption to the hydrophobic polymer surface. This constant is temperature-dependent, but the dependency does not follow a monotonic trend. In particular, Eugenio et al. [70] found a peak in the k_{cat} value near Tg, but the absorption constant (K) was lower. The value is also dependent on medium conditions, such as the solvent surface tension; Bååth et al. [60] tested the non-ionic surfactant DDM, which had a mixed effect, because it increased the rate constant but diminished the affinity, as there was a reduction in Γ_{attack}. This was explained as an accumulation of the surfactant molecules on the substrate surface. Non-ionic detergents reduce accessible sites. Additional alternatives are the construction of chimeras with PET binding domains, but the effect of these modifications on the $^{molar}\eta$ must be experimentally assayed, because this parameter determines the enzyme's ability to reach complete degradation in shorter times. Furukawa et al. [74] treated the PET surface with anionic surfactants of varying chain lengths, which enhanced their interaction with *Is*PETase, resulting in a significant increase in TPA production when PET film was incubated with sodium tetradecyl sulfate (C_{14}–$OSO3^-$) for 1 h. Bååth et al. [75] found that adding different concentrations of the cationic surfactant cetyltrimethylammonium bromide (CTAB), affected substrate binding strength and turnover. They observed relationships between these factors, expressed by the Sabatier principle of moderate enzyme-substrate affinity for interfacial enzymes: PET hydrolysis was better when the interaction was intermediate in strength under steady-state conditions and unrestrained diffusion. More experimental work is needed to evaluate mass transfer and temperature effects, from the perspective of the Sabatier principle.

The temperature dependency of the reaction allows an estimation of the activation energies for the enzymatic and chemical hydrolysis of the polymer. There are studies on HiC [70], and the enzyme does not cause a drastic reduction in the energy barrier of the transition state at the limiting chemical step. There is still room for improvement for these catalysts.

3.1.2. Thermostability

It is possible to improve thermal stability (i.e., a higher Tm of the enzyme), by creating new interactions, such as introducing disulfide or salt bridges, stabilizing or introducing a metal binding site, glycosylation sites, or using co-solvents [46,47,51,67,76,77].

- Ions and co-solvents

Ronkvist et al. [46] depolymerized PET film in the presence of co-solvent, and 10% glycerol protected HiC from thermal inactivation. The reaction reached almost 100% weight loss in 96 h, at 70 °C. Nevertheless, HiC could not depolymerize biaxially oriented (bo) PET under the same reaction conditions. Kawai et al. [78] changed 24% glycerol for 10% EG, improving PET hydrolysis with a variant of Cut190.

An alternative is using eco-friendly deep eutectic solvents (DES), which could both enhance the protein's thermal stability and improve PET enzymatic hydrolysis. At the same time, DES could increase the access to PET cleavable sites, under enzymatic reaction conditions [79–81].

On the other hand, the thermal stability of some cutinases from actinomycetes was improved by the addition of divalent ions, such as Ca^{2+} or Mg^{2+}. In the case of Ca^{2+}, site- directed mutagenesis of the binding sites in Cut190 showed that one was involved in enzyme activation, while the other two increased the protein thermal stability [47,67,82–84].

Other cutinase orthologs showed similar behavior with these ions [85]. Kawai et al. [47] evaluated the Cut190 variant S226P/R228S, and found a 5 °C increase in Tm with 300 mM $CaCl_2$ and 24% glycerol, enhancing the activity and TPA yield, at 63 °C. Divalent cations also enhanced PET film degradation by the *Thermobifida fusca* enzyme [85], and improved the Tm of PHL7 [49].

- Design of disulfide bridges

Then et al. [86] introduced disulfide and salt bridges in TfCut2, using three mutations (D204C/E253C/D174R). In addition, Oda et al. [67] designed an enzyme introducing five mutations in Cut190 (Q138A/D250C-E296C/Q123H/N202H). In both cases, the mutations resulted in an increased Tm. The Cut190 variant degraded GF-PET by more than 30%, without any evidence of product inhibition, at 70 °C. Furthermore, to enhance the thermostability of LCC, Tournier et al. [87] introduced a disulfide bridge at the divalent-metal-binding site, formed by E208, D238, and S283 [88], by the mutations D238C/S283C. Then the Tm increased by 9.8 °C, compared to wild-type enzyme (84.7 °C), as verified by differential scanning fluorimetry. However, the enzyme lost 28% hydrolytic activity against PET. Similar results were found by some other authors [50,54,89,90]. This behavior can be explained, since an important factor in an enzyme's enhancement of reaction rates lies in its molecular dynamics during catalysis, then, if enhanced stability reduces protein motion, it may slow down the rate-limiting catalytic step [91].

- Other stabilizing mutations

In addition, the development of better computational algorithms to aid protein engineering has resulted in improvements in Tm and the activity of several enzymes.

Not long ago, some authors [51,89,92–95] increased the thermal stability of *Is*PETase and improved its depolymerization activity. They generated variants with Tm values from 1.1 to 31 °C higher than the wild-type *Is*PETase, and they introduced new interactions into the *Is*PETase enzyme molecule, the best variant of *Is*PETase was named "FAST-PETase", designed with the aid of machine learning software [51]. These biocatalysts have activity towards amorphous PET. Besides, Zeng et al. [96] evaluated some mutations, and the best variant was LCC-ICCG-RIP (A59R/V63I/N248P), having a Tm of 98 °C. This enzyme depolymerized PET samples at temperatures ranging between 74 to 85 °C, with the variant exhibiting higher activity than the original enzyme LCC-ICCG, in that temperature range.

Recently, Wu et al. [97] deposited data from their work in progress at Research Square, where they redesigned a variant of BhrPETase (H218S/F222I/A209R/D238K/A251C/A281C/W104L/F243T) by deep learning. This biocatalyst has enhanced activity 4.4-fold, compared to the wild-type, with a Tm of 84 °C, and depolymerizes PET with a productivity of 77.3 g_{TPAeq} L^{-1} h^{-1}, at 300 g L^{-1} PET suspension, making it an attractive enzyme for bio-recycling, even though it was not able to digest highly crystalline PET.

3.1.3. Catalytic Efficiency

To date, some crystallographic structures of cutinases and PETases are available on the Protein Data Bank (PDB) archive, from free native or engineered enzymes, or from their complexes with HEMT, MHET, or BHET. These crystal structures have given some insight into how the substrate interacts with these proteins. However, crystal structures of complexes with longer oligomers may be necessary to understand the role of enzyme-substrate interactions along the substrate-binding cleft [50,57,96,98]. Furthermore, to get a complete picture, these data need to be complemented with studies of enzyme kinetics and catalytic properties, and structural studies, with tools such as NMR [14,53,60,70,88,99,100]. In fact, an overwhelming amount of structural data may soon be available, since the DeepMind company revealed their intention to predict all the structures in the entire UniRef100 database, using the artificial intelligence software "AlphaFold 2.0" [101]. More recently, DeepMind released AlphaFill [102], a software that may expand the current knowledge of PETases–PET complexes, and provide theoretical enzyme–ligand models, to

fill in the structural gap. Nevertheless, there are limited reports offering a detailed kinetic characterization of these enzymes.

Some researchers predicted the modes of binding of a model substrate, using in silico molecular docking and molecular dynamics simulations, and compared several enzyme homologs. Wei et al. [68] analyzed some TfCut2 variants. From their in silico data, some amino acid residues were selected, according to predicted interactions with 2PET, and were compared to the LCC structure using structural alignment. Then, with site-directed mutagenesis, they produced the single G62A and double G62A/I213S variants, which improved the degradation of PET film from 15.9 to 42.6% weight loss, after 50 h, at 65 °C, as compared to the wild-type enzyme. The gain in degradation achieved by the G62A mutant was ascribed to the enhanced catalytic activity and a reduced binding affinity for MHET. In later research, Furukawa et al. [103] compared the sequence of TfCut2 from *T. fusca* with *Is*PETase, identified non-conserved amino acid residues around the active site, and then designed the variants G62A [68], H129W, F209S, and F209A. All of them made the enzyme between 1.5 to 2.9-fold more active than the wild-type, against PET sheets. They studied the concomitant effect of the mutations and observed three double variants (G62A/H129W, G62A/F209S, and G62A/F209A) with higher hydrolytic activity than wild-type and single variants. The most interesting variant was the double mutant G62A/F209A, displaying the highest activity, due to the modification of the substrate-binding cleft. Unfortunately, when they analyzed the effect of high crystallinity, they observed a very low activity against this kind of substrate, a result that shows this bottleneck is still a challenge.

Herrero Acero et al. [104] described variants of Thc_Cut2 from *T. cellulosilytica* DSM44535, revealing the role of amino acid residues on the enzyme surface, for PET hydrolysis. Their sequence similarity analysis showed two superficially divergent regions in Thc_Cut1 compared to Thc_Cut2. The variant Thc_Cut2 (R29N/A30V, in region 1) was cloned and expressed in *E. coli*, and this variant released TPA at a higher level than the wild-type Thc_Cut1 and Thc_Cut2. A stabilizing effect was observed on the surface of region 1, exerted by stronger hydrophobic interactions, a cavity size reduction, and a reduced superficial positive charge. Tournier et al. [87] identified some essential amino acid residues by molecular docking of the model substrate 2-HE$(MHET)_3$. The most active variants were the replacement of F243 by I or W. However, the activity was sensitive to temperature, which led to the combination of the variants F243I/D238C/S283C (ICC) and F243W/D238C/S283C (WCC), to produce variants with 122% and 98% residual activity, while their Tm increased by 6.2 °C and 10.1 °C, respectively. Finally, variants F243I/D238C/S283C/Y127G (ICCG) and F243W/D238C/S283C/Y127G (WCCG), also had improved activity, and increased Tm by 9.3 °C and 13.4 °C, respectively. The best variant to hydrolyze Pf-PET was F243I (104.4 $mg_{TAeq}.h^{-1}.mg_{enzyme}{}^{-1}$), compared to the wild-type. In summary, these results point to surface charge balance and hydrophobicity as key factors to consider, in the rational engineering of effective PETases.

Recently, Zhang et al. [54] reanalyzed Thc_Cut1 for PC-PET depolymerization. They compared it with TfCut2 and LCC cutinases, and tested the double mutation G63A/F210I, which had an enhanced PET conversion into TPA:MHET 2:1, after 96 h, at 60 °C. The mutations expanded the substrate-binding cleft of Thc_Cut1, mimicking the one in the engineered cutinase from *Fusarium solani* [58]. Moreover, the performance of Thc_Cut1 was improved by introducing a disulfide bridge, so they designed the variant G63A/F210I/D205C7E254C/Q93G. However, when used against PC-PET, the polymer lost 96% of the initial weight in 96 h, at 70 °C, producing mainly TPA.

In a more recent study, Lu et al. [51] redesigned *Is*PETase (S121E/D186H/R280A/R224Q/N233K) based on the artificial intelligence software MutCompute (see above, under, other stabilizing mutations), seeking to improve the catalytic activity at moderate temperatures. In contrast to other works, this group focused on an enzyme able to attack PET samples at ambient temperature, because such an enzyme could be used to decompose PET in contaminated natural ecosystems. The resulting PETase showed high activity, releasing TPA and MHET after 96 h reaction time, at 50 °C. The improvements were explained by:

(i) the formation of an intramolecular salt bridge between N233K and E204; (ii) the R224Q mutation formed a new hydrogen bond with the carbonyl group of the S192 mutation; and (iii) S121E building a new water-mediated hydrogen-bonding network with H186 and N172. All these amino acid residues are far from the catalytic S160, yet their effects on the catalytic properties of the enzyme are significant. This contribution illustrates the implicit difficulties in the rational design of enzymes, but it is also very promising because it shows how artificial intelligence computational tools can impact this field. This enzyme, named FAST-PETase, was able to depolymerize 51 samples (1.18–6.24% crystallinity), including a water bottle, with amorphous and highly crystalline parts. From the results, the amorphous sections were completely degraded to monomers, while highly crystalline zones released traces of mixed products, confirming the hampering of enzymatic hydrolysis by high-crystallinity PET. The obstacle could be solved by thermal pretreatment, i.e., melting the whole bottle, followed by a quick cooling, to turn most of the sample amorphous (2% crystallinity). With more recalcitrant samples, the periodic addition of fresh medium was found to be a requirement to achieve nearly complete degradation, probably due to enzyme inactivation and product inhibition. Unfortunately, the ratio of TPA, MHET, and BHET in the product mix was not reported, but the wild-type *Is*PETase was reported to release MHET and TPA, in the range from 1.3:1 to 1.6:1 [41,42,57], while for the *Is*PETase derivative ThermoPETase, a value of 2.2:1 was reported [105]. The relative proportion of products is an important issue to be considered in this line of research, because the specific application's protocols may greatly benefit from the use of enzyme mixtures. This is a hint given to us by nature, as for instance, *Ideonella sakaiensis* 201-F6 produces a two-enzyme system, consisting of *Is*PETase and *Is*MHETase, which improves the TPA yield [24].

LCC-ICCG was co-crystallized with MHET. The enzyme-substrate complex showed a minimal conformational change compared to the apo-form (Cα RMSD 0.317 Å), it bonded ready for catalytic reaction, however, it accumulated MHET, and its hydrolysis was slow. Some studies have found hydrolases having high K_M and small k_{cat} for MHET [24,95,106]. Charlier et al. [88] studied the interaction between MHET and different variants of LCC, to understand the improved properties of LCC-ICCG. Using NMR chemical shift perturbations (CSP), they identified regions of the proteins where MHET interacted. Some residues were rigid, but they induced changes either far away, or close to, the active site, with different concentrations of MHET. Perhaps an enthalpy–entropy compensation or entropy–entropy compensation, with some contribution by the solvent [107], is stabilizing the complex. More experimental evidence is needed, using different NMR methods, isothermal titration calorimetry (ITC) with different enzymes, and the investigation of the physicochemical properties of substrates like MHET, BHET, and PET, under the reaction conditions. The relationship between the complex enzyme-substrate and the solvent seems particularly relevant to this aim [108]. Chen et al. [109] found interesting mutations in *Thermobifida fusca* cutinase, and designed the variant H184S/Q92G/F209I/I213K, which exhibited 30-fold more activity against PET than the wild-type. They evaluated these mutations in LCC and BhrPETase enzymes. Both increased TPA production and produced a low amount of MHET. Perhaps H218S and S247K mutations could have a synergistic effect in LCC-ICCG, to enhance MHET hydrolysis. Recently, Schubert et al. [73] and Brizendine et al. [110], found MHET to undergo autohydrolysis. Thus, enhancing MHET's autohydrolysis rate would be enough to minimize product inhibition, and this could, perhaps, be attained with subtle changes to the reaction medium or conditions.

3.1.4. Search for Novel PET Hydrolases

The phylogenetic analysis of known PET hydrolases, has revealed more enzymes with possible activity against PET present in nature. Erickson et al. [111] identified potential thermostable PET hydrolases using bioinformatic tools, machine learning, X-rays, and AlphaFold. They found enzymes with different folds, substrate-binding cleft properties, and active site architectures, that depolymerized highly crystalline, amorphous, and PET film in the ranges 30–70 °C and pH 6–9. These new enzymes are limited to polyesterase,

lipase, and cutinase enzymes, with different residues in the substrate-binding cleft, which could enhance hydrolytic activity against PET samples.

Figure 3 shows the structural alignment of different enzymes reported in the UniRef100 database and their reported mutation hot spots. The figure points to eight positions around the active site cleft, which influence the enzyme properties, and the potential for mutations is immense.

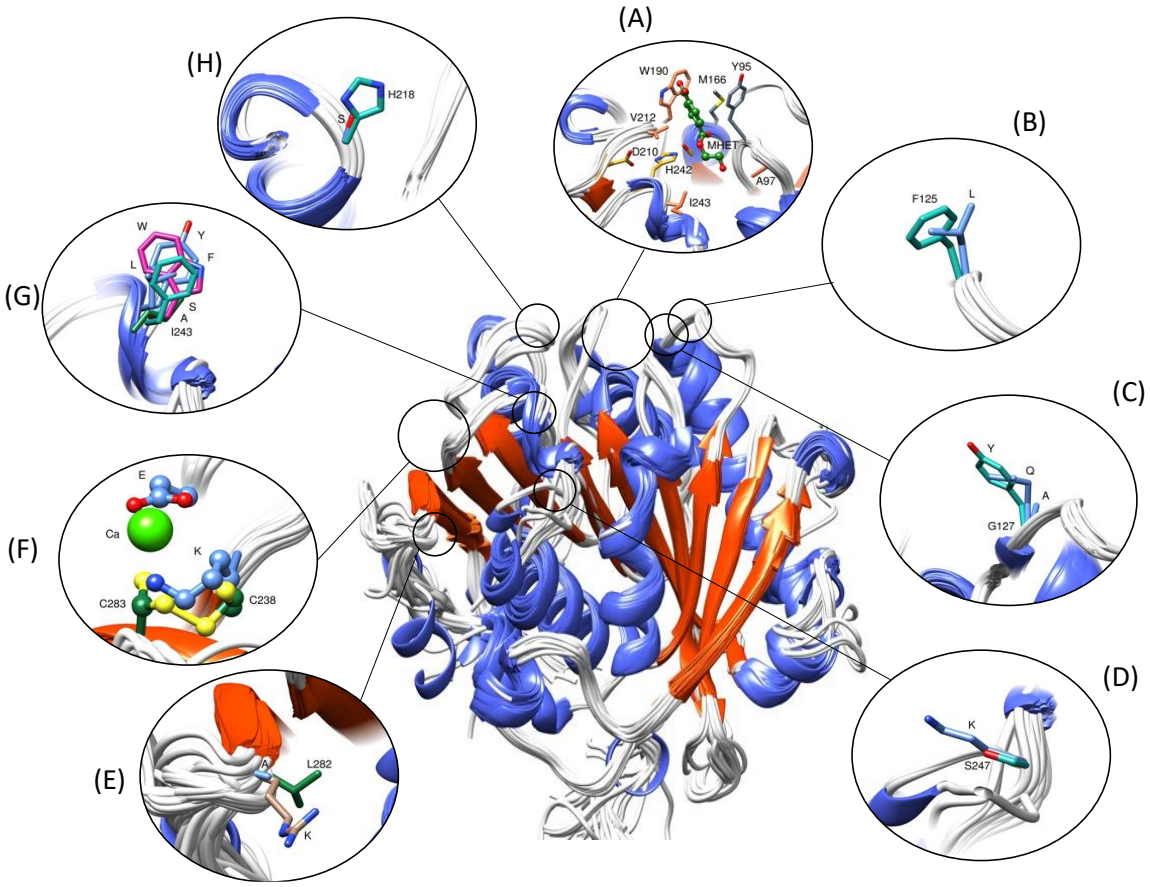


Figure 3. Some mutation hot spots were documented on the superposed crystal structures, with 3D models created by AlphaFold 2.0 (Supplementary Table S1), of known hydrolases. The backbone of the LCC-ICCG complex with MHET (7VVE), was superposed with other homologs. (**A**) The catalytic triad (S165, H242, and D210), oxyanion holes (Y95, M166), and residues that contributed to the MHET binding (W190, V212, I243, H242, H164, A97, M166, and Y95) [96]. (**B**) F125 is a possible target to mutate; Leucine is present in another PET hydrolase [50]. (**C**) G197 is a mutation hot spot, equivalent to Y197 in LCC [112], A138 [78], and Q94 [50]. (**D**) S247 is a residue far from the active site, changed to lysine [109]. (**E**) L282 is a distant residue from the active site, equivalent to a lysine in *Is*PETase [41], and mutated to alanine [42]. (**F**) Strategies to improve thermostability: a disulfide bridge C238–C283 [87], a metal binding site [67], and a salt bridge [51]. (**G**) One frequent mutation hot spot is I243, equivalent to Phe [112], Leu [50], Ser [41] in other proteins, and it has been mutated to Ala [9,103], Tyr [113], and Trp [87]. (**H**) H218 is close to the active site and was mutated to Ser [109].

Even assuming one residue per each site indicated in Figure 3, there might be 8 single mutants, 28 combinations taking two sites at a time, 56 taking three, 70 taking four, 56 taking five, 28 taking six, 8 taking seven sites, and one if we change all eight sites. Then, for single mutants, there can be 19 substitutions for each site, giving 152 possibilities, while with two sites there can be 361 possible residue substitutions for each of the 28 combinations, leading to 10,108 potential double variants. Extending the analysis to three, four, five, six,

seven, and eight sites, there could be roughly 25.6 billion variants to be explored. Clearly, the potential for innovation is far from exhausted.

3.1.5. Enzyme Combinations and Chimeras to Solve MHET Hydrolysis

Barth et al. [69] evaluated a dual system LCC or TfCut2, with a carboxylesterase from *Thermobifida fusca* KW3, covalently immobilized. The best performance was LCC/carboxylesterase, which yielded more than twice as much TPA than TfCut2/carboxylesterase. On the other hand, de Castro et al. [114] reported synergy in the PC-PET hydrolysis by *Moesziomyces antarcticus* (formerly *Candida antarctica*) lipase B (CALB) with HiC, releasing over four times more TPA than MHET plus BHET, at 50 °C. These two enzymes, used sequentially, achieved the depolymerization of a water bottle and amorphous PET. Digestion with HiC, followed by treatment with CALB, resulted in 3.6 times more TPA than MHET, but these yields were dependent on the origin of PET and its crystallinity. These strategies improved TPA yields, but MHET concentration was still significant, which can increase bio-recycling costs. Therefore, MHET accumulation is an issue worth considering.

Knott et al. [106] optimized a dual system of *Is*PETase and *Is*MHETase, acting on GF-PET. According to these authors, *Is*PETase:*Is*MHETase:GF-PET in a proportion 0.002:0.001:1 (w:w:w), achieved the best results. This combination yielded 1.5 mM of TPA, free of detectable BHET or MHET (by HPLC). The performance of the enzyme mix was synergistic, compared to the performance of single enzymes. The success of these authors, led to the design of chimeras fusing *Is*MHETase to *Is*PETase, with several flexible glycine-serine linkers of 8, 12, and 20 amino acid residues. The chimeric protein MP20 (with a 20-residues-long linker), resulted in the highest yield of TPA, as compared to IsPETase, *Is*MHETase, or their mix in the proportion to PET 0.00025:0.0005:1 (w:w:w), although optimal reaction conditions were not really explored. The strategy is attractive, because it improves the yields of the products of interest (TPA and EG), it only invests in the production of one enzyme, and could make the whole process more profitable. A similar approach has been taken with chimeras of a lipase and a cutinase (Lip-Cut), for the efficient enzymatic removal of ink from waste paper [115] and the degradation of poly (ε-caprolactone) [116].

To enhance polymer interaction, some authors designed and evaluated enzyme-binding modules fused. Ribitsch et al. [117] studied the effect of the fusion of binding domains in Thc_Cut1, the binding module from cellobiohydrolase I, from *Hypocrea jecorina* (CBM), and from a polyhydroxyalkanoate depolymerase, from *Alcaligenes faecalis* (PBM), on the adsorption and hydrolysis of PET film. Thc_Cut1 fused with PBM hydrolyzed PET film better than a mixture of the separate CBM and the free Thc_Cut1. Weber et al. [118] evaluated eight different CBMs, to determine which adsorbs better onto the surface of PET nanoparticles. The most promising was BaCBM2 module, binding with a K_d of 25.4 mg/L. In addition, Xue et al. [119] analyzed the effect of different binding modules fused to the C terminus of the LC-cutinase ICCG variant. They found that the ChBD and CBM modules improved hydrolysis compared to the independent enzymes, with CBM being the most promising, depolymerizing almost 100% of the PET after 12 h.

There are reports of chimeras designed to degrade PET and MHET, by combining thermostable and highly active domains [120,121]. This sounds appealing, as it may improve TPA yield, if each component prefers a different form of PET.

4. Strategies to Improve Biocatalyst-Polymer Interaction and Monomers Yield

The first step for the hydrolysis of PET is the adsorption of the biocatalyst on the polymer surface, being a critical point for degradation [59–62]. Bååth et al. [53] determined the binding parameters of Thc_Cut1 and Thc_Cut2 from binding isotherms. These cutinases share a similar maximal binding capacity, and there are only minor differences in their K_d. Thc_Cut2 displayed higher affinity than Thc_Cut1, at 60 °C. On the other hand, Badino et al. [61] studied the PET binding of three PET hydrolases (HiC, TfCut2, and *Is*PETase) and found K_d values between 12 and 61 nM, at 40 °C, respectively, and this changed with temperature. Surprisingly, these authors did not evaluate the K_d at

temperatures closer to Tg, where HiC and TfCut2 display higher activity. The binding capacity of the PET surface determined in this study corresponds to a protein monolayer. Non-specific interactions predominantly direct the adsorption under the conditions evaluated. Nevertheless, the K_d values of the enzymes were of the same order of magnitude (nM) as that observed for cellulases adsorbing to cellulose, by specific interactions of their carbohydrate-binding modules.

Since the PET surface is hydrophobic, using hydrophobins could improve the protein–PET interaction and enhance its hydrolysis. Puspitasari et al. [122] studied the interaction of class 1 hydrophobin RolA, from *Aspergillus oryzae*, and HGFI from *Grifola frondose*, with *Is*PETase and PET. RolA and HGFI, applied as PET pretreatment, decreased the water contact angle (WCA). After the pretreatment of PET fiber with hydrophobins, the subsequent depolymerization of PET samples was better than when only *Is*PETase was used. However, again, and against expectations, the crystallinity had a negative effect on the degradation.

In a pioneering study, Vogel et al. [62] investigated the interaction between TfCut2 and nanoparticles of PET, using ITC in combination with a thermokinetic model. They found an enthalpy of surface adsorption of –129 kJ mol^{-1} ($\Delta_{Ads}H$), an enthalpy for ester-bond cleavage of -58 kJ mol^{-1} ($\Delta_{EB}H$), and the apparent dissociation constant of the enzyme-substrate complex was 0.046 g L^{-1}. Then, 95% of the heat exchange during PET depolymerization was due to the bond-breaking enthalpy and only 5% was adsorption heat. ITC allowed the clear breakdown of the mass transfer and bond-breaking contributions to the reaction thermodynamics, which is a critical piece of information to consider in the understanding and engineering of PET degradation [123,124]. Furthermore, with appropriate kinetic and thermodynamic models, ITC allows the study of PET–enzyme interactions in multiphasic systems. Even with biocatalysts attacking PET with low efficiency, some may bind well to the polymer surface, thus offering valuable information to improve the mass transfer properties of PET hydrolases. As mentioned before, engineering of chimeras, by combining good binding domains with powerful bond-breaking, or catalytic domains, can be done. Then, different flexible linkers may be tested to keep the protein closer to the polymer surface for more time and increase the probability of productive enzyme-substrate collisions. More studies are needed in this poorly explored area, perhaps using as a reference, the in-depth exploration of the kinetics of cellulase acting on lignocellulosic materials [125,126].

4.1. PET Pretreatment

So far, there is no biocatalyst that efficiently hydrolyzes highly crystalline PET, if applied directly to a bottle for a bio-recycling process. Thus, different strategies may be required to increase ester bond accessibility and enhance protein adsorption. In some reports [50,51,87], the authors were able to degrade crystalline PET after a treatment to reduce the number of crystalline PET regions. So, pretreatments are currently useful for complete bio-recycling.

High temperature has been the pretreatment of choice in many reports [50,51,87]. A common finding is a need for careful temperature control, since mechanical stress, caused by local temperature gradients, increases crystallinity [10,50,127]. In addition, temperature treatments may be combined with grinding, as in cryo-milling [78,110] and in thermomechanical pretreatment [87]. Unfortunately, even after enzymatic treatment, a prolonged heating exposure at 70 °C provokes physical aging and induces rigid polymer microstructures [14,67,87]. In this sense, physical changes of PET microstructures may be a complicating factor, frequently disregarded in studies of enzyme activity and stability against temperature. Further studies are required, to analyze the composition of microstructures before and after the reaction [10,78]. It has been shown that cleavage of X_{MAF} by thermomechanical degradation tended to lead to its reorganization into X_{RAF}. Furthermore, X_C was formed earlier and more rapidly after each reprocessing [128]. Clearly, this is a factor deserving more attention.

Other pretreatment strategies include, using solvents and detergents to increase the accessibility of cleavable sites. Carniel et al. [129] soaked PC-PET in MEG, followed by washing with Tween 80 and then distilled water. TPA recovery was substantially improved, due to a positive effect on the enzyme-substrate interaction. Additional treatments make use of mechanical forces, such as ultrasound or grinding. Pellis et al. [130] used Thc_Cut1 to degrade PET powder, with ultrasonic treatment for different periods. They found a direct relationship between the crystalline PET content and the sonication time required. As expected, the ultrasonic treatment turned out to be less effective for PET films, where the exposed surface is considerably smaller. The ultrasound treatment could change the polymer structure, so more studies with calorimetry, IR, and NMR methods are needed, to characterize the effects of these treatments. Gamerith et al. and Castro et al. [59,71] have provided good evidence of an improvement of TPA release caused by a reduction of the particle size of PET, but found a strong effect of crystalline zones, since a PET sample with a high crystallinity content was poorly degraded, even at tiny particle sizes [50,59,87,114]. Brizendine et al. [110] provided very good evidence of this problem, by using sieves to separate CM-PET and HC-PET particles in PET powder, and digesting these samples with LCC-ICCG. The TPA yield was considerably higher for CM-PET-rich particles, while in HC-PET the degradation products included more MHET and the TPA yield was low. One major complication in the analysis of these studies lies in the variation in enzyme sources, mixing strategies, and reaction conditions used in these reports, because problems such as product inhibition may not affect all enzymes in the same way [69], and mass transfer may be increased by stirring [70].

Atmospheric plasma non-thermal pretreatment of the PET surface, exposes hydroxyl (-OH) and carboxylic (-COOH) terminal groups, and increases PET hydrophilicity. Therefore, the water contact angle was changed from 141° to 0° [131]. This plasma technology is a low-cost process, that might be combined with PET hydrolases to depolymerize PET. In addition, there are some plasma capable reactors, for example, discharge of dielectric barrier and plasma photocatalyst [131,132]. These could well be useful for PET pretreatment.

4.2. Effect of Reaction Medium

The information available on the solvent's role in the enzyme–PET binding and catalysis is still limited. From a thermodynamic point of view, the solvent plays a critical role. In the literature, we can find some examples of how the reaction medium impacts the reaction product profiles. Schmidt et al. [133] evaluated the effect of several buffers (MOPS, sodium phosphate, and Tris) at different concentrations (0.1–1 M). LCC lost activity at MOPS or TRIS concentrations higher than 0.1 M, although LCC remained stable in concentrated sodium phosphate buffer. Phosphate buffer at high concentration did not reduce depolymerization activity at temperatures near the Tg [49,50,70,76,134]. On the other hand, Carniel et al. and Eugenio et al. [135,136] evaluated the PC-PET hydrolysis reaction using different reaction mediums and HiC. In a Tris-HCl buffer, the reaction yielded mainly TPA, while in alkaline water and sodium phosphate buffer, HiC released TPA, MHET, and BHET.

4.3. Mass Transfer Problems

In the studies included in this review, orbital shakers, hybrid incubators, and thermomixers are used to agitate reaction vessels. Only in recent years, have trials been scaled up to the reactor level, with a gain in mass and heat transfer efficiency, due to improved geometrical design, the inclusion of impellers, physical barriers present, and sensors to monitor and control different variables in real-time, such as pH and temperature. Some aspects related to process engineering will be discussed below.

Castro et al. [59] used a stirred bioreactor, with two sets of impellers with Rushton blades, to improve TPA yield and shorten degradation times. Some authors [110,113,119] also found a benefit from using a similar Rushton and single marine impeller [87], to improve the degradation of PET samples with high crystallinity and small surface exposure.

Other authors also studied pH changes in the reactor, and found these to be a relevant factor [59,87,110,113,135,136]. According to these groups, a pH-stat in the reactor can change the proportion of different products, and, with appropriate conditions, the TPA yield can be improved preferentially [135]. Mass transfer [59,70,87,110,113,119,135,136], pH control [50,59,78,87,110,113,135,136], PET suspension [59,70,87,110,113,119,135,136], and temperature [59,70,87,110,113,119,135,136] also affected product mixtures and their yields, and these suggest that more detailed physicochemical studies are still needed.

In all the previous works, the amount of enzyme was also considered an essential factor [59,70,87,110,113,119,135,136], both for technical reasons and for its economic impact. An additional factor to consider would be continuous product removal [59,70,87,110,113, 119,134–136], because products act as reaction inhibitors. This product removal should be achieved, preferably, with enzyme retention in the reaction, to make the whole process more efficient and economical. In this sense, significant work on engineering the degradation in reactors is still pending. An increase in monomer yields was observed when all concomitant factors explained in this section were evaluated in PET hydrolysis, as shown in Table 1. Some of these factors were optimized by the French biotechnological company CARBIOS, and they reached 90% depolymerization of PET waste in 10 h, generating TPA and EG [87]. They were able to scale-up their process to a 20 m^3 reactor, allowing the degradation of almost 20 tons of PET waste, with a productivity of 15 g_{TPA} L^{-1} h^{-1}. The recovered, purified monomers were then used to synthetize new PET resin [137]. Singh et al. [138] have recently produced an excellent analysis of the economy of PET degradation and recycling. Their analysis laid a significant weight of the profitability into feedstock pretreatment, enzymatic PET depolymerization, and product or co-product recovery. This analysis showed that the cost of enzymatic PET recycling might be competitive with virgin PET resin costs. Comparing reaction conditions between chemical and enzymatic degradation, the latter is moderated, temperature and pressure are lower than chemical degradation, and it is friendly to the environment. Bio-recycling products is valuable and, as mentioned before, useful to create new products in a circular economy. However, there is still room to improve the process and enhance productivity. The process works well for amorphous PET, however, there is not any enzyme that is able to completely digest highly crystalline PET. This could decrease the cost of the process, leaving behind PET extrusion and micronization preprocessing to reduce crystallinity.

Table 1. Depolymerization of PET samples by PET hydrolases.

Source	Enzyme	Substrate	Reaction Conditions	TPA (mM)	Productivity (mgTPA L^{-1} h^{-1})	Reference
Idonella sakaiensis	PETase	PET film C [c]	T [d], B [d], pH 7.2, 50 nM, 96 h time reaction	0.511	0.88	[41]
	PETase-W159H/S238F			0.421	0.42	
	Chimera *Is*MHETase/*Is*PETase-MP20	GF-PET C [d]	T [d], B [d], pH 7.5, 10% DMSO, 96 h reaction time	1.5	2.6	[106]
	*Is*PETase-S121E/D186H/R280A/R224Q/N233K	19 g_{GF-PET} L^{-1} C [d]	T [c], B [c], pH 8, 200 nM, 96 h reaction time	33.8 [a]	58.49 [a]	[51]
Humicola insolens	Novozym® 51032	20 g_{PET} L^{-1} C [c]	T [b], B [b], A [c], pH 7, 10 $mg_{protein}$ $g_{PET}{}^{-1}$, 336 h reaction time	~45	~22.25	[114]
		20 g_{PET} L^{-1} C [b]		~0.450	~0.22	
		81 g_{PC-PET} L^{-1} C [b]	T [b], B [b], A [b], pH 8.95, 65 $mg_{protein}$ $g_{PET}{}^{-1}$, 96 h reaction time	64	110.75	[59]
		81 g_{PC-PET} L^{-1} C [b]	T [c], B [b], A [b], pH 8.95, 32 $mg_{protein}$ $g_{PET}{}^{-1}$, 96 h reaction time	96.54	47.73	[135]
		220 g_{PC-PET} L^{-1} C [b]	T [b], B [b], A [b], pH 7, 1 $mg_{protein}$ mL^{-1}, 96 h reaction time	105.6	182.74	[70]

Table 1. *Cont.*

Source	Enzyme	Substrate	Reaction Conditions	TPA (mM)	Productivity (mgTPA L^{-1} h^{-1})	Reference
Metagenome from leaf branch compost	LCC	25 g_{PET} L^{-1}	T [b], B [c], pH 8, 5 µg enzyme, 24 h reaction time	28	193.82	[112,139]
	LCC-F243I/D238C/S283C/Y127G	200 $g_{PC\text{-}PET}$ kg^{-1} C [c]	T [b], B [c], A [b], pH 8, 3 mg_{enzyme} g_{PET}^{-1}, 9.3 h reaction time	935 [a]	16,702.32 [a]	[87]
	LCC-F243I/D238C/S283C/Y127G	0.6 $g_{GF\text{-}PET}$ L^{-1} C [d]	T [b], B [c], A [b], pH 8, 0.5 µmol enzyme, 12 h reaction time	0.76	10.52	[119]
	LCC-F243I/D238C/S283C/Y127G-CBM			1.23	17.03	
	LCC-F243I/D238C/S283C/Y127G	100 $g_{LC\text{-}PET}$ L^{-1} C [d]	T [b], B [c], A [b], pH 8, 3 mg_{ICCG} g_{PET}^{-1}, 144 h reaction time	475	548	[110]
		100 $g_{WC\text{-}PET}$ L^{-1} C [c]		124.9	144.09	
		100 $g_{HC\text{-}PET}$ L^{-1} C [b]		100	115.37	
	LCC-F243Y/D238C/S283C/Y127G	200 $g_{GF\text{-}PET}$ L^{-1} C [d]	T [b], B [c], A [b], pH 7.5, 12.5 mM enzyme, 96 h reaction time	953	1649	[113]
	LCC-F243Y/D238C/S283C/Y127G-*Tr*CBM1			829	1435	
Metagenome compost	PHL7	83 $g_{GF\text{-}PET}$ L^{-1} C [d]	T [b], B [b], A [c], pH 8, 0.6 mg_{enzyme} g_{PET}^{-1}, 16 h reaction time	~95	~986.4	[49]
	PES-H1	PET powder C [c]	T [b], B [b], A [c], pH 8, 1 mg_{enzyme} g_{PET}^{-1}, 24 h reaction time	~75	~519.16	[50]
	PES-H1-L92F/Q94Y			~200	~1384.42	
Thermobifida fusca	TfCut2	PET nanoparticle	T [b], B [b], A [c], pH 8.5, 50 µg mL^{-1} enzyme, 24 h reaction time	0.6	4.15	[66]
		GF-PET C [d]	T [b], B [b], A [b], pH 8, 18 µg mL^{-1} enzyme, 24 h reaction time	12	83.07	[134]
Thermobifida cellulosilytica	Thc_Cut2	20 g_{PET} L^{-1} C [b]	T [b], B [c], A [c], pH 8, 18 µg mL^{-1} enzyme, 30 h reaction time	~0.018	~0.1	[53]
	Thc_Cut1	50 g_{PET} L^{-1} C [b]	T [b], B [b], A [c], pH 8, 5 µM enzyme, 96 h reaction time	55	95.18	[76]
	Thc_Cut1_koST			62	107.29	
	Thc_Cut1-G63A/F210I/D205C/E254C/Q93G	8.3 $g_{GF\text{-}PET}$ L^{-1} C [d]	T [b], B [c], A [c], pH 8, 75 µg enzyme, 96 h reaction time	34.7	60.05	[54]
Saccharomonospora viridis	Cut190Q138A/D250C-E296C/Q123H/N202H	GF-PET C [d]	T [b], B [c], pH 8.2, 2 µM enzyme, 72 h reaction time	15 [a]	34.61 [a]	[67,140]
	Cut190**SS/L136F/Q138G/F255I *	20 g_{PET}/L C [d]	T [b], B [c], A [c], pH 9, 2 µM enzyme, 72 h reaction time	94.9 [a]	218.97 [a]	[78]

[a] Data calculated with the sum of products TPA, BHET, or MHET concentration. [b] Harsh conditions: Temperature (T) ≥ 60 °C, stirred bioreactor (A), buffer concentration (B) ≥200 mM, PET crystallinity (C) ≥20%. [c] Moderate conditions: Temperature (T) 50–59 °C, agitation in incubator or ThermoMixer (A), buffer concentration (B) ≥100 mM, PET crystallinity (C) ≥10–19%. [d] Gentle conditions: Temperature (T) < 50 °C, buffer concentration (B) ≤ 50 mM, PET crystallinity (C) < 10%.* Cut190**SS is equivalent to variantQ138A/S226P/R228S/D250C-E296C/Q123H/N202H/K305del/L306del/N307del, which leads to the introduction of an additional disulphide bond.

5. Challenges and Perspectives

The PET hydrolysis reaction is a complex system, in which many factors influence the efficiency of the recovery of TPA and EG monomers. The interaction between the enzyme and PET occurs as follows: (1) The enzyme is found within the bulk of the reaction medium and collides with the PET surface by diffusion mechanisms. (2) The biocatalyst adsorbs to the polyester surface, in a nonspecific manner, through hydrophobic interactions, π-stacking, hydrogen bonds, and electrostatic interactions. (3) The biocatalyst–PET complex is formed. (4) Catalysis occurs and oligomers are released into the bulk reaction medium. The depolymerization starts as an endo- or exo-hydrolytic process, and may change at longer times [52,73,78]. (5) The biocatalyst desorbs from the polyester surface. (6) There is a

homogeneous catalysis within the bulk reaction medium, as the concentration of the degradation products increases, as shown in Figure 4. Most PET hydrolyzing enzymes have a high affinity for the PET surface and a high specificity constant for the ester bond present in the polyester, but under steady-state conditions, an intermediate binding strength increases the rate of PET hydrolysis. Many parameters already discussed in this review influence the hydrolysis of PET, such as reaction temperature, enzyme activity, thermostability and concentration of the biocatalyst, pretreatment of the PET, the amount of suspended PET, the size of the PET particle, its molecular mass, the crystallinity and microstructures of the PET sample, the reaction medium, the pH and its control during the reaction, reaction time, mixing efficiency, and mass and heat transfer. However, one question remains: Is it possible to hydrolyze an untreated PET sample, with crystallinity over 20%, by directly applying an enzyme?

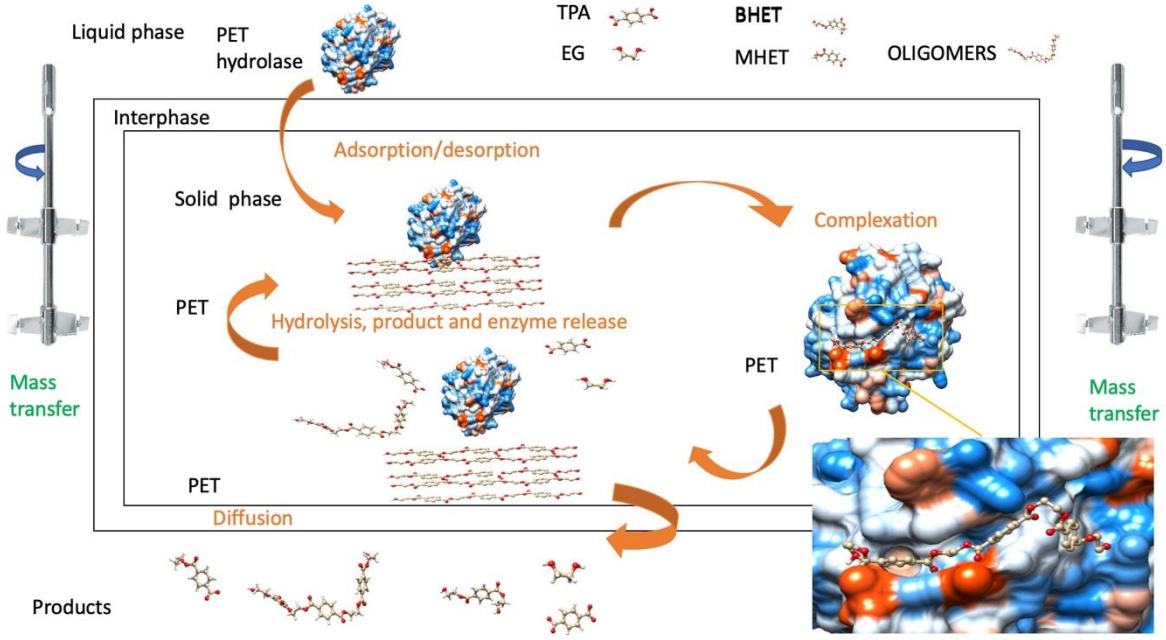


Figure 4. Scheme of the main steps of the mechanism of interaction and depolymerization between PET hydrolases and PET, improved by mass transfer.

More studies are required to understand the mechanisms to depolymerize highly crystalline PET and to grasp the physicochemical properties of the different substrates (MHET, BHET, and PET), as they are produced during the degradation process, under different reaction conditions. To achieve an efficient depolymerization of PET, thermostable enzymes, selective for *gauche* and *trans* conformations [9], and having high specific constants, may be required, to deal with crude PET samples. Finally, the field should benefit from a standard protocol, to assay new enzymes and their variants against PET, BHET, and MHET. Currently, comparisons are complicated by the diversity in experimental approaches.

In future research, the study of hydrolysis with enzyme chimeras with more than one catalytic domain is proposed, along with enzymes fused to high-affinity carbohydrate-binding modules in bioreactors, where there is better control of mass transfer and the reaction parameters. Besides, the hydrolysis of PET in bioreactors, using unconventional reaction media such as DES, should be explored. Furthermore, hydrolysis in different geometries and types of bioreactors, such as percolate ones, should be studied. The effect of pressure in pressurized and reduced pressure bioreactors, to increase the yield of monomers and cut down costs, is a condition to be explored. In addition, the protocols to recover enzymes from the reaction mixture are underdeveloped, and it would be interesting to assess for how long the enzymes retain their properties and catalytic proficiency. Finally, further developments in artificial intelligence tools may open the door to the design of

"hallucinated" enzymes, which do not exist and have never existed in nature [141]. Tools like Alphafold [142], RoseTTAfold [143], ProteinMPNN [144], and other tools [145,146], have already yielded completely novel enzyme folds, but the sequence space of proteins is overwhelmingly large and nature has only explored a tiny fraction of it, because the number of combinations theoretically possible is many orders of magnitude larger than the total mass in the universe times its total estimated age. Perhaps a few of these hallucinated enzymes may fully depolymerize PET to its monomers TPA and EG, in a short time, and with a high yield.

Supplementary Materials: The following supporting information can be downloaded at: https://www.mdpi.com/article/10.3390/catal13030591/s1, Table S1: Example of homologs of PET hydrolases.

Author Contributions: Conceptualization, J.A.C.-R., R.R.-S. and A.F.; methodology, J.A.C.-R. and R.R.-S.; software, J.A.C.-R. and R.R.-S.; validation, J.A.C.-R. and R.R.-S.; formal analysis, J.A.C.-R. and R.R.-S.; investigation, J.A.C.-R. and R.R.-S.; resources, A.F.; data curation, J.A.C.-R. and R.R.-S.; writing—original draft preparation, J.A.C.-R.; writing—review and editing, R.R.-S. and A.F.; visualization, J.A.C.-R. and R.R.-S.; supervision, A.F.; project administration, A.F.; funding acquisition, A.F. All authors have read and agreed to the published version of the manuscript.

Funding: This review was funded by PAIP 5000-9095 FACULTAD DE QUIMICA PAPIIT IN 201921 DGAPA, JACR is recipient of CONACYT scholarship 750551 and CVU 661660.

Data Availability Statement: This study did not report any data.

Conflicts of Interest: The authors declare no conflict of interest.

References

1. Plastics—The Facts 2022. 2022. Available online: https://plasticseurope.org/wp-content/uploads/2022/10/PE-PLASTICS-THE-FACTS_V7-Tue_19-10-1.pdf (accessed on 6 November 2022).
2. Gasperi, J.; Wright, S.L.; Dris, R.; Collard, F.; Mandin, C.; Guerrouache, M.; Langlois, V.; Kelly, F.J.; Tassin, B. Microplastics in Air: Are We Breathing It In? *Curr. Opin. Environ. Sci. Health* **2018**, *1*, 1–5. [CrossRef]
3. Suaria, G.; Achtypi, A.; Perold, V.; Lee, J.R.; Pierucci, A.; Bornman, T.G.; Aliani, S.; Ryan, P.G. Microfibers in Oceanic Surface Waters: A Global Characterization. *Sci. Adv.* **2020**, *6*, eaay8493. [CrossRef] [PubMed]
4. Karami, A.; Golieskardi, A.; Keong Choo, C.; Larat, V.; Galloway, T.S.; Salamatinia, B. The Presence of Microplastics in Commercial Salts from Different Countries. *Sci. Rep.* **2017**, *7*, 46173. [CrossRef] [PubMed]
5. Bhuyan, M.S. Effects of Microplastics on Fish and in Human Health. *Front. Environ. Sci.* **2022**, *10*, 827289. [CrossRef]
6. Aguilar-Guzmán, J.C.; Bejtka, K.; Fontana, M.; Valsami-Jones, E.; Villezcas, A.M.; Vazquez-Duhalt, R.; Rodríguez-Hernández, A.G. Polyethylene Terephthalate Nanoparticles Effect on RAW 264.7 Macrophage Cells. *Microplastics Nanoplastics* **2022**, *2*, 9. [CrossRef]
7. MacLeod, M.; Arp, H.P.H.; Tekman, M.B.; Jahnke, A. The Global Threat from Plastic Pollution. *Science* **2021**, *373*, 61–65. [CrossRef]
8. Papadopoulou, A.; Hecht, K.; Buller, R. Enzymatic PET Degradation. *Chimia* **2019**, *73*, 743–749. [CrossRef]
9. Guo, B.; Vanga, S.R.; Lopez-Lorenzo, X.; Saenz-Mendez, P.; Ericsson, S.R.; Fang, Y.; Ye, X.; Schriever, K.; Bäckström, E.; Biundo, A.; et al. Conformational Selection in Biocatalytic Plastic Degradation by PETase. *ACS Catal.* **2022**, *12*, 3397–3409. [CrossRef]
10. Thomsen, T.B.; Hunt, C.J.; Meyer, A.S. Influence of Substrate Crystallinity and Glass Transition Temperature on Enzymatic Degradation of Polyethylene Terephthalate (PET). *New Biotechnol.* **2022**, *69*, 28–35. [CrossRef]
11. Zimmermann, W. Biocatalytic Recycling of Polyethylene Terephthalate Plastic: Biocatalytic Plastic Recycling. *Philos. Trans. R. Soc. A Math. Phys. Eng. Sci.* **2020**, *378*, 20190273. [CrossRef]
12. Kawai, F.; Kawabata, T.; Oda, M. Current State and Perspectives Related to the Polyethylene Terephthalate Hydrolases Available for Biorecycling. *ACS Sustain. Chem. Eng.* **2020**, *8*, 8894–8908. [CrossRef]
13. Carniel, A.; de Abreu Waldow, V.; de Castro, A.M. A Comprehensive and Critical Review on Key Elements to Implement Enzymatic PET Depolymerization for Recycling Purposes. *Biotechnol. Adv.* **2021**, *52*, 107811. [CrossRef] [PubMed]
14. Wei, R.; Breite, D.; Song, C.; Gräsing, D.; Ploss, T.; Hille, P.; Schwerdtfeger, R.; Matysik, J.; Schulze, A.; Zimmermann, W. Biocatalytic Degradation Efficiency of Postconsumer Polyethylene Terephthalate Packaging Determined by Their Polymer Microstructures. *Adv. Sci.* **2019**, *6*, 1900491. [CrossRef]
15. Panowicz, R.; Konarzewski, M.; Durejko, T.; Szala, M.; Łazi, M. Properties of Polyethylene Terephthalate (PET) after Thermo-Oxidative Aging. *Materials* **2021**, *14*, 3833. [CrossRef] [PubMed]
16. Lens-Pechakova, L.S. Recent Studies on Enzyme-Catalysed Recycling and Biodegradation of Synthetic Polymers. *Adv. Ind. Eng. Polym. Res.* **2021**, *4*, 151–158. [CrossRef]
17. Kushwaha, A.; Goswami, L.; Singhvi, M.; Kim, B.S. Biodegradation of Poly(Ethylene Terephthalate): Mechanistic Insights, Advances, and Future Innovative Strategies. *Chem. Eng. J.* **2023**, *457*, 141230. [CrossRef]

18. Ghosal, K.; Nayak, C. Recent Advances in Chemical Recycling of Polyethylene Terephthalate Waste into Value Added Products for Sustainable Coating Solutions—Hope vs. Hype. *Mater. Adv.* **2022**, *3*, 1974–1992. [CrossRef]
19. Sovová, K.; Ferus, M.; Matulková, I.; Španěl, P.; Dryahina, K.; Dvořák, O.; Civiš, S. A Study of Thermal Decomposition and Combustion Products of Disposable Polyethylene Terephthalate (PET) Plastic Using High Resolution Fourier Transform Infrared Spectroscopy, Selected Ion Flow Tube Mass Spectrometry and Gas Chromatography Mass Spectrometr. *Mol. Phys.* **2008**, *106*, 1205–1214. [CrossRef]
20. Jung, K.W.; Kim, J.H.; Choi, J.W. Synthesis of Magnetic Porous Carbon Composite Derived from Metal-Organic Framework Using Recovered Terephthalic Acid from Polyethylene Terephthalate (PET) Waste Bottles as Organic Ligand and Its Potential as Adsorbent for Antibiotic Tetracycline Hydrochlo. *Compos. Part B Eng.* **2020**, *187*, 107867. [CrossRef]
21. Yang, Q.; Li, H.; Wang, D.; Zhang, X.; Guo, X.; Pu, S.; Guo, R.; Chen, J. Utilization of Chemical Wastewater for CO_2 Emission Reduction: Purified Terephthalic Acid (PTA) Wastewater-Mediated Culture of Microalgae for CO_2 Bio-Capture. *Appl. Energy* **2020**, *276*, 115502. [CrossRef]
22. Zhou, J.; Sun, J.; Ullah, M.; Wang, Q.; Zhang, Y.; Cao, G.; Chen, L.; Ullah, M.W.; Sun, S. Polyethylene Terephthalate Hydrolysate Increased Bacterial Cellulose Production. *Carbohydr. Polym.* **2023**, *300*, 120301. [CrossRef] [PubMed]
23. Malafatti-Picca, L.; de Barros Chaves, M.R.; de Castro, A.M.; Valoni, É.; de Oliveira, V.M.; Marsaioli, A.J.; de Franceschi de Angelis, D.; Attili-Angelis, D. Hydrocarbon-Associated Substrates Reveal Promising Fungi for Poly (Ethylene Terephthalate) (PET) Depolymerization. *Braz. J. Microbiol.* **2019**, *50*, 633–648. [CrossRef] [PubMed]
24. Yoshida, S.; Hiraga, K.; Takehana, T.; Taniguchi, I.; Yamaji, H.; Maeda, Y.; Toyohara, K.; Miyamoto, K.; Kimura, Y.; Oda, K. A Bacterium That Degrades and Assimilates Poly(Ethylene Terephthalate). *Science* **2016**, *353*, 759. [CrossRef] [PubMed]
25. Gong, J.; Kong, T.; Li, Y.; Li, Q.; Li, Z.; Zhang, J. Biodegradation of Microplastic Derived from Poly(Ethylene Terephthalate) with Bacterial Whole-Cell Biocatalysts. *Polymers* **2018**, *10*, 1326. [CrossRef] [PubMed]
26. Asmita, K.; Shubhamsingh, T.; Tejashree, S. Isolation of Plastic Degrading Micro-Organisms from Soil Samples Collected at Various Locations in Mumbai, India. *Int. Res. J. Environ. Sci.* **2015**, *4*, 77–85.
27. Khoironi, A.; Anggoro, S.; Sudarno, S. Evaluation of the Interaction Among Microalgae *Spirulina sp*, Plastics Polyethylene Terephthalate and Polypropylene in Freshwater Environment. *J. Ecol. Eng.* **2019**, *20*, 161–173. [CrossRef]
28. Dąbrowska, G.B.; Janczak, K.; Richert, A. Combined Use of *Bacillus* Strains and Miscanthus for Accelerating Biodegradation of Poly(Lactic Acid) and Poly(Ethylene Terephthalate). *PeerJ* **2021**, *9*, e10957. [CrossRef]
29. Huang, Q.S.; Yan, Z.F.; Chen, X.Q.; Du, Y.Y.; Li, J.; Liu, Z.Z.; Xia, W.; Chen, S.; Wu, J. Accelerated Biodegradation of Polyethylene Terephthalate by *Thermobifida fusca* Cutinase Mediated by *Stenotrophomonas pavanii*. *Sci. Total Environ.* **2022**, *808*, 152107. [CrossRef]
30. Dhaka, V.; Singh, S.; Ramamurthy, P.C.; Samuel, J.; Swamy Sunil Kumar Naik, T.; Khasnabis, S.; Prasad, R.; Singh, J. Biological Degradation of Polyethylene Terephthalate by *Rhizobacteria*. *Environ. Sci. Pollut. Res.* **2022**. [CrossRef]
31. Farzi, A.; Dehnad, A.; Fotouhi, A.F. Biodegradation of Polyethylene Terephthalate Waste Using *Streptomyces* Species and Kinetic Modeling of the Process. *Biocatal. Agric. Biotechnol.* **2019**, *17*, 25–31. [CrossRef]
32. Qi, X.; Ma, Y.; Chang, H.; Li, B.; Ding, M.; Yuan, Y. Evaluation of PET Degradation Using Artificial Microbial Consortia. *Front. Microbiol.* **2021**, *12*, 778828. [CrossRef] [PubMed]
33. Chen, Z.; Wang, Y.; Cheng, Y.; Wang, X.; Tong, S.; Yang, H.; Wang, Z. Efficient Biodegradation of Highly Crystallized Polyethylene Terephthalate through Cell Surface Display of Bacterial PETase. *Sci. Total Environ.* **2020**, *709*, 136138. [CrossRef] [PubMed]
34. Chen, Z.; Duan, R.; Xiao, Y.; Wei, Y.; Zhang, H.; Sun, X.; Wang, S.; Cheng, Y.; Wang, X.; Tong, S.; et al. Biodegradation of Highly Crystallized Poly(Ethylene Terephthalate) through Cell Surface Codisplay of Bacterial PETase and Hydrophobin. *Nat. Commun.* **2022**, *13*, 7138. [CrossRef] [PubMed]
35. Zhu, B.; Ye, Q.; Seo, Y.; Wei, N. Enzymatic Degradation of Polyethylene Terephthalate Plastics by Bacterial Curli Display PETase. *Environ. Sci. Technol. Lett.* **2022**, *9*, 650–657. [CrossRef]
36. Yan, F.; Wei, R.; Cui, Q.; Bornscheuer, U.T.; Liu, Y.J. Thermophilic Whole-Cell Degradation of Polyethylene Terephthalate Using Engineered *Clostridium thermocellum*. *Microb. Biotechnol.* **2021**, *14*, 374–385. [CrossRef]
37. Kawai, F.; Kawabata, T.; Oda, M. Current Knowledge on Enzymatic PET Degradation and Its Possible Application to Waste Stream Management and Other Fields. *Appl. Microbiol. Biotechnol.* **2019**, *103*, 4253–4268. [CrossRef]
38. Chen, S.; Su, L.; Chen, J.; Wu, J. Cutinase: Characteristics, Preparation, and Application. *Biotechnol. Adv.* **2013**, *31*, 1754–1767. [CrossRef]
39. Martínez, A.; Maicas, S. Cutinases: Characteristics and Insights in Industrial Production. *Catalysts* **2021**, *11*, 1194. [CrossRef]
40. Xi, X.; Ni, K.; Hao, H.; Shang, Y.; Zhao, B.; Qian, Z. Secretory Expression in *Bacillus subtilis* and Biochemical Characterization of a Highly Thermostable Polyethylene Terephthalate Hydrolase from *Bacterium* HR29. *Enzym. Microb. Technol.* **2021**, *143*, 109715. [CrossRef]
41. Austin, H.P.; Allen, M.D.; Donohoe, B.S.; Rorrer, N.A.; Kearns, F.L.; Silveira, R.L.; Pollard, B.C.; Dominick, G.; Duman, R.; Omari, K.E.; et al. Characterization and Engineering of a Plastic-Degrading Aromatic Polyesterase. *Proc. Natl. Acad. Sci. USA* **2018**, *115*, E4350–E4357. [CrossRef]
42. Joo, S.; Cho, I.J.; Seo, H.; Son, H.F.; Sagong, H.Y.; Shin, T.J.; Choi, S.Y.; Lee, S.Y.; Kim, K.J. Structural Insight into Molecular Mechanism of Poly(Ethylene Terephthalate) Degradation. *Nat. Commun.* **2018**, *9*, 382. [CrossRef] [PubMed]
43. Chen, C.C.; Han, X.; Ko, T.P.; Liu, W.; Guo, R.T. Structural Studies Reveal the Molecular Mechanism of PETase. *FEBS J.* **2018**, *285*, 3717–3723. [CrossRef] [PubMed]

44. Chen, C.C.; Han, X.; Li, X.; Jiang, P.; Niu, D.; Ma, L.; Liu, W.; Li, S.; Qu, Y.; Hu, H.; et al. General Features to Enhance Enzymatic Activity of Poly(Ethylene Terephthalate) Hydrolysis. *Nat. Catal.* **2021**, *4*, 425–430. [CrossRef]
45. Müller, R.J.; Schrader, H.; Profe, J.; Dresler, K.; Deckwer, W.D. Enzymatic Degradation of Poly(Ethylene Terephthalate): Rapid Hydrolyse Using a Hydrolase from *T. Fusca*. *Macromol. Rapid Commun.* **2005**, *26*, 1400–1405. [CrossRef]
46. Ronkvist, Å.M.; Xie, W.; Lu, W.; Gross, R.A. Cutinase-Catalyzed Hydrolysis of Poly(Ethylene Terephthalate). *Macromolecules* **2009**, *42*, 5128–5138. [CrossRef]
47. Kawai, F.; Oda, M.; Tamashiro, T.; Waku, T.; Tanaka, N.; Yamamoto, M.; Mizushima, H.; Miyakawa, T.; Tanokura, M. A Novel Ca2+-Activated, Thermostabilized Polyesterase Capable of Hydrolyzing Polyethylene Terephthalate from *Saccharomonospora viridis* AHK190. *Appl. Microbiol. Biotechnol.* **2014**, *98*, 10053–10064. [CrossRef] [PubMed]
48. Sulaiman, S.; Yamato, S.; Kanaya, E.; Kim, J.J.; Koga, Y.; Takano, K.; Kanaya, S. Isolation of a Novel Cutinase Homolog with Polyethylene Terephthalate-Degrading Activity from Leaf-Branch Compost by Using a Metagenomic Approach. *Appl. Environ. Microbiol.* **2012**, *78*, 1556–1562. [CrossRef]
49. Sonnendecker, C.; Oeser, J.; Richter, P.K.; Hille, P.; Zhao, Z.; Fischer, C.; Lippold, H.; Blázquez-Sánchez, P.; Engelberger, F.; Ramírez-Sarmiento, C.A.; et al. Low Carbon Footprint Recycling of Post-Consumer PET Plastic with a Metagenomic Polyester Hydrolase. *ChemSusChem* **2022**, *15*, e202101062. [CrossRef]
50. Pfaff, L.; Gao, J.; Li, Z.; Jäckering, A.; Weber, G.; Mican, J.; Chen, Y.; Dong, W.; Han, X.; Feiler, C.G.; et al. Multiple Substrate Binding Mode-Guided Engineering of a Thermophilic PET Hydrolase. *ACS Catal.* **2022**, *12*, 9790–9800. [CrossRef]
51. Lu, H.; Diaz, D.J.; Czarnecki, N.J.; Zhu, C.; Kim, W.; Shroff, R.; Acosta, D.J.; Alexander, B.R.; Cole, H.O.; Zhang, Y.; et al. Machine Learning-Aided Engineering of Hydrolases for PET Depolymerization. *Nature* **2022**, *604*, 662–667. [CrossRef]
52. Herrero Acero, E.; Ribitsch, D.; Steinkellner, G.; Gruber, K.; Greimel, K.; Eiteljoerg, I.; Trotscha, E.; Wei, R.; Zimmermann, W.; Zinn, M.; et al. Enzymatic Surface Hydrolysis of PET: Effect of Structural Diversity on Kinetic Properties of Cutinases from *Thermobifida*. *Macromolecules* **2011**, *44*, 4632–4640. [CrossRef]
53. Arnling Bååth, J.; Novy, V.; Carneiro, L.V.; Guebitz, G.M.; Olsson, L.; Westh, P.; Ribitsch, D. Structure-Function Analysis of Two Closely Related Cutinases from *Thermobifida cellulosilytica*. *Biotechnol. Bioeng.* **2022**, *119*, 470–481. [CrossRef] [PubMed]
54. Zhang, Z.; Huang, S.; Cai, D.; Shao, C.; Zhang, C.; Zhou, J.; Cui, Z.; He, T.; Chen, C.; Chen, B.; et al. Depolymerization of Post-Consumer PET Bottles with Engineered Cutinase 1 from *Thermobifida cellulosilytica*. *Green Chem.* **2022**, *24*, 5998–6007. [CrossRef]
55. Wyeth, N.C.; Mendenhall, P.; Roseveare, R.N. Biaxially Oriented Poly(Ethylene Terephthalate) Bottle. United States Patent US3733309A, 3 September 1985.
56. Witt, U.; Müller, R.-J.; Augusta, J.; Widdecke, H.; Deckwer, W.-D. Synthesis, Properties and Biodegradability of Polyesters Based on 1,3-Propanediol. *Macromol. Chem. Phys.* **1994**, *195*, 793–802. [CrossRef]
57. Han, X.; Liu, W.; Huang, J.W.; Ma, J.; Zheng, Y.; Ko, T.P.; Xu, L.; Cheng, Y.S.; Chen, C.C.; Guo, R.T. Structural Insight into Catalytic Mechanism of PET Hydrolase. *Nat. Commun.* **2017**, *8*, 1–6. [CrossRef]
58. Araújo, R.; Silva, C.; O'Neill, A.; Micaelo, N.; Guebitz, G.; Soares, C.M.; Casal, M.; Cavaco-Paulo, A. Tailoring Cutinase Activity towards Polyethylene Terephthalate and Polyamide 6,6 Fibers. *J. Biotechnol.* **2007**, *128*, 849–857. [CrossRef]
59. De Castro, A.M.; Carniel, A.; Stahelin, D.; Junior, L.S.C.; de Angeli Honorato, H.; de Menezes, S.M.C. High-Fold Improvement of Assorted Post-Consumer Poly(Ethylene Terephthalate) (PET) Packages Hydrolysis Using *Humicola insolens* Cutinase as a Single Biocatalyst. *Process Biochem.* **2019**, *81*, 85–91. [CrossRef]
60. Bååth, J.A.; Borch, K.; Jensen, K.; Brask, J.; Westh, P. Comparative Biochemistry of Four Polyester (PET) Hydrolases**. *ChemBioChem* **2021**, *22*, 1627–1637. [CrossRef]
61. Badino, S.F.; Bååth, J.A.; Borch, K.; Jensen, K.; Westh, P. Adsorption of Enzymes with Hydrolytic Activity on Polyethylene Terephthalate. *Enzym. Microb. Technol.* **2022**, *152*, 109937. [CrossRef]
62. Vogel, K.; Wei, R.; Pfaff, L.; Breite, D.; Al-Fathi, H.; Ortmann, C.; Estrela-Lopis, I.; Venus, T.; Schulze, A.; Harms, H.; et al. Enzymatic Degradation of Polyethylene Terephthalate Nanoplastics Analyzed in Real Time by Isothermal Titration Calorimetry. *Sci. Total Environ.* **2021**, *773*, 145111. [CrossRef]
63. Scandola, M.; Focarete, M.L.; Frisoni, G. Simple Kinetic Model for the Heterogeneous Enzymatic Hydrolysis of Natural Poly(3-Hydroxybutyrate). *Macromolecules* **1998**, *31*, 3846–3851. [CrossRef]
64. Aer, L.; Jiang, Q.; Gul, I.; Qi, Z.; Feng, J.; Tang, L. Overexpression and Kinetic Analysis of *Ideonella sakaiensis* PETase for Polyethylene Terephthalate (PET) Degradation. *Environ. Res.* **2022**, *212*, 113472. [CrossRef] [PubMed]
65. Reuveni, S.; Urbakh, M.; Klafter, J. Role of Substrate Unbinding in Michaelis-Menten Enzymatic Reactions. *Proc. Natl. Acad. Sci. USA* **2014**, *111*, 4391–4396. [CrossRef]
66. Barth, M.; Oeser, T.; Wei, R.; Then, J.; Schmidt, J.; Zimmermann, W. Effect of Hydrolysis Products on the Enzymatic Degradation of Polyethylene Terephthalate Nanoparticles by a Polyester Hydrolase from *Thermobifida fusca*. *Biochem. Eng. J.* **2015**, *93*, 222–228. [CrossRef]
67. Oda, M.; Yamagami, Y.; Inaba, S.; Oida, T.; Yamamoto, M.; Kitajima, S.; Kawai, F. Enzymatic Hydrolysis of PET: Functional Roles of Three Ca2+ Ions Bound to a Cutinase-like Enzyme, Cut190*, and Its Engineering for Improved Activity. *Appl. Microbiol. Biotechnol.* **2018**, *102*, 10067–10077. [CrossRef]

68. Wei, R.; Oeser, T.; Schmidt, J.; Meier, R.; Barth, M.; Then, J.; Zimmermann, W. Engineered Bacterial Polyester Hydrolases Efficiently Degrade Polyethylene Terephthalate Due to Relieved Product Inhibition. *Biotechnol. Bioeng.* **2016**, *113*, 1658–1665. [CrossRef] [PubMed]
69. Barth, M.; Honak, A.; Oeser, T.; Wei, R.; Belisário-Ferrari, M.R.; Then, J.; Schmidt, J.; Zimmermann, W. A Dual Enzyme System Composed of a Polyester Hydrolase and a Carboxylesterase Enhances the Biocatalytic Degradation of Polyethylene Terephthalate Films. *Biotechnol. J.* **2016**, *11*, 1082–1087. [CrossRef]
70. Eugenio, E.D.Q.; Campisano, I.S.P.; de Castro, A.M.; Coelho, M.A.Z.; Langone, M.A.P. Kinetic Modeling of the Post-Consumer Poly(Ethylene Terephthalate) Hydrolysis Catalyzed by Cutinase from *Humicola insolens*. *J. Polym. Environ.* **2021**, *30*, 1627–1637. [CrossRef]
71. Gamerith, C.; Zartl, B.; Pellis, A.; Guillamot, F.; Marty, A.; Acero, E.H.; Guebitz, G.M. Enzymatic Recovery of Polyester Building Blocks from Polymer Blends. *Process Biochem.* **2017**, *59*, 58–64. [CrossRef]
72. Pirillo, V.; Pollegioni, L.; Molla, G. Analytical Methods for the Investigation of Enzyme-Catalyzed Degradation of Polyethylene Terephthalate. *FEBS J.* **2021**, *288*, 4730–4745. [CrossRef]
73. Schubert, S.; Schaller, K.; Bååth, J.A.; Hunt, C.; Borch, K.; Jensen, K.; Brask, J.; Westh, P. Reaction Pathways for the Enzymatic Degradation of Poly(Ethylene Terephthalate): What Characterizes an Efficient PET-Hydrolase? *ChemBioChem* **2022**, *24*, e202200516. [CrossRef] [PubMed]
74. Furukawa, M.; Kawakami, N.; Oda, K.; Miyamoto, K. Acceleration of Enzymatic Degradation of Poly(Ethylene Terephthalate) by Surface Coating with Anionic Surfactants. *ChemSusChem* **2018**, *11*, 4018–4025. [CrossRef] [PubMed]
75. Baath, J.A.; Jensen, K.; Borch, K.; Westh, P.; Kari, J. Sabatier Principle for Rationalizing Enzymatic Hydrolysis of a Synthetic Polyester. *J. Am. Chem. Soc.* **2022**, *2*, 1223–1231. [CrossRef]
76. Gamerith, C.; Vastano, M.; Ghorbanpour, S.M.; Zitzenbacher, S.; Ribitsch, D.; Zumstein, M.T.; Sander, M.; Acero, E.H.; Pellis, A.; Guebitz, G.M. Enzymatic Degradation of Aromatic and Aliphatic Polyesters by *P. Pastoris* Expressed Cutinase 1 from *Thermobifida cellulosilytica*. *Front. Microbiol.* **2017**, *8*, 938. [CrossRef]
77. Shirke, A.N.; White, C.; Englaender, J.A.; Zwarycz, A.; Butterfoss, G.L.; Linhardt, R.J.; Gross, R.A. Stabilizing Leaf and Branch Compost Cutinase (LCC) with Glycosylation: Mechanism and Effect on PET Hydrolysis. *Biochemistry* **2018**, *57*, 1190–1200. [CrossRef]
78. Kawai, F.; Furushima, Y.; Mochizuki, N.; Muraki, N.; Yamashita, M.; Iida, A.; Mamoto, R.; Tosha, T.; Iizuka, R.; Kitajima, S. Efficient Depolymerization of Polyethylene Terephthalate (PET) and Polyethylene Furanoate by Engineered PET Hydrolase Cut190. *AMB Express* **2022**, *12*, 134. [CrossRef]
79. Wang, Q.; Yao, X.; Geng, Y.; Zhou, Q.; Lu, X.; Zhang, S. Deep Eutectic Solvents as Highly Active Catalysts for the Fast and Mild Glycolysis of Poly(Ethylene Terephthalate)(PET). *Green Chem.* **2015**, *17*, 2473–2479. [CrossRef]
80. Tan, Y.; Henehan, G.T.; Kinsella, G.K.; Ryan, B.J. Cutinase from *Amycolatopsis mediterannei*: Marked Activation and Stabilisation in Deep Eutectic Solvents. *Bioresour. Technol. Rep.* **2021**, *16*, 100882. [CrossRef]
81. Attallah, O.A.; Azeem, M.; Nikolaivits, E.; Topakas, E.; Fournet, M.B. Microwave-Assisted Green Deep Eutectic Solvent and Enzymatic Treatment. *Polymers* **2022**, *14*, 109. [CrossRef]
82. Kawabata, T.; Oda, M.; Kawai, F. Mutational Analysis of Cutinase-like Enzyme, Cut190, Based on the 3D Docking Structure with Model Compounds of Polyethylene Terephthalate. *J. Biosci. Bioeng.* **2017**, *124*, 28–35. [CrossRef]
83. Numoto, N.; Kamiya, N.; Bekker, G.J.; Yamagami, Y.; Inaba, S.; Ishii, K.; Uchiyama, S.; Kawai, F.; Ito, N.; Oda, M. Structural Dynamics of the PET-Degrading Cutinase-like Enzyme from *Saccharomonospora viridis* AHK190 in Substrate-Bound States Elucidates the Ca2+-Driven Catalytic Cycle. *Biochemistry* **2018**, *57*, 5289–5300. [CrossRef] [PubMed]
84. Inaba, S.; Kamiya, N.; Bekker, G.J.; Kawai, F.; Oda, M. Folding Thermodynamics of PET-Hydrolyzing Enzyme Cut190 Depending on Ca 2+ Concentration. *J. Therm. Anal. Calorim.* **2019**, *135*, 2655–2663. [CrossRef]
85. Then, J.; Wei, R.; Oeser, T.; Barth, M.; Belisário-Ferrari, M.R.; Schmidt, J.; Zimmermann, W. Ca2+ and Mg2+ Binding Site Engineering Increases the Degradation of Polyethylene Terephthalate Films by Polyester Hydrolases from *Thermobifida fusca*. *Biotechnol. J.* **2015**, *10*, 592–598. [CrossRef]
86. Then, J.; Wei, R.; Oeser, T.; Gerdts, A.; Schmidt, J.; Barth, M.; Zimmermann, W. A Disulfide Bridge in the Calcium Binding Site of a Polyester Hydrolase Increases Its Thermal Stability and Activity against Polyethylene Terephthalate. *FEBS Open Bio* **2016**, *6*, 425–432. [CrossRef]
87. Tournier, V.; Topham, C.M.; Gilles, A.; David, B.; Folgoas, C.; Moya-Leclair, E.; Kamionka, E.; Desrousseaux, M.-L.; Texier, H.; Gavalda, S.; et al. An Engineered PET Depolymerase to Break down and Recycle Plastic Bottles. *Nature* **2020**, *580*, 216–219. [CrossRef] [PubMed]
88. Charlier, C.; Gavalda, S.; Borsenberger, V.; Duquesne, S.; Marty, A.; Tournier, V.; Lippens, G. An NMR Look at an Engineered PET Depolymerase. *Biophys. J.* **2022**, *121*, 2882–2894. [CrossRef] [PubMed]
89. Brott, S.; Pfaff, L.; Schuricht, J.; Schwarz, J.-N.; Böttcher, D.; Badenhorst, C.P.S.; Wei, R.; Bornscheuer, U.T. Engineering and Evaluation of Thermostable IsPETase Variants for PET Degradation. *Eng. Life Sci.* **2022**, *22*, 192–203. [CrossRef] [PubMed]
90. Emori, M.; Numoto, N.; Senga, A.; Bekker, G.-J.; Kamiya, N.; Kobayashi, Y.; Ito, N.; Kawai, F.; Oda, M. Structural Basis of Mutants of PET-Degrading Enzyme from *Saccharomonospora viridis* AHK190 with High Activity and Thermal Stability. *Proteins Struct. Funct. Bioinforma.* **2021**, *89*, 502–511. [CrossRef]

91. Sampedro, J.G.; Uribe, S. Trehalose-Enzyme Interactions Result in Structure Stabilization and Activity Inhibition. The Role of Viscosity. *Mol. Cell. Biochem.* **2004**, *256*, 319–327. [CrossRef]
92. Cui, Y.; Chen, Y.; Liu, X.; Dong, S.; Tian, Y.Y.; Qiao, Y.; Mitra, R.; Han, J.; Li, C.; Han, X.; et al. Computational Redesign of a PETase for Plastic Biodegradation under ambient condition by the GRAPE Strategy. *ACS Catal.* **2021**, *11*, 1340–1350. [CrossRef]
93. Meng, X.; Yang, L.; Liu, H.; Li, Q.; Xu, G.; Zhang, Y.; Guan, F.; Zhang, Y.; Zhang, W.; Wu, N.; et al. Protein Engineering of Stable IsPETase for PET Plastic Degradation by Premuse. *Int. J. Biol. Macromol.* **2021**, *180*, 667–676. [CrossRef] [PubMed]
94. Rennison, A.; Winther, J.R.; Varrone, C. Rational Protein Engineering to Increase the Activity and Stability of Ispetase Using the Pross Algorithm. *Polymers* **2021**, *13*, 3884. [CrossRef] [PubMed]
95. Yin, Q.; You, S.; Zhang, J.; Qi, W.; Su, R. Enhancement of the Polyethylene Terephthalate and Mono-(2-Hydroxyethyl) Terephthalate Degradation Activity of *Ideonella sakaiensis* PETase by an Electrostatic Interaction-Based Strategy. *Bioresour. Technol.* **2022**, *364*, 128026. [CrossRef]
96. Zeng, W.; Li, X.; Yang, Y.; Min, J.; Huang, J.W.; Liu, W.; Niu, D.; Yang, X.; Han, X.; Zhang, L.; et al. Substrate-Binding Mode of a Thermophilic PET Hydrolase and Engineering the Enzyme to Enhance the Hydrolytic Efficacy. *ACS Catal.* **2022**, *12*, 3033–3040. [CrossRef]
97. Wu, B.; Cui, Y.; Chen, Y.; Sun, J.; Zhu, T.; Li, C.; Geng, W. Deep Learning-Aided Redesign of a Hydrolase for near 100% PET Depolymerization under Industrially Relevant Conditions. *Research Square.* **2023**. (*preprint*). [CrossRef]
98. Li, Z.; Zhao, Y.; Wu, P.; Wang, H.; Li, Q.; Gao, J.; Qin, H.M.; Wei, H.; Bornscheuer, U.T.; Han, X.; et al. Structural Insight and Engineering of a Plastic Degrading Hydrolase Ple629. *Biochem. Biophys. Res. Commun.* **2022**, *626*, 100–106. [CrossRef] [PubMed]
99. Wei, R.; Song, C.; Gräsing, D.; Schneider, T.; Bielytskyi, P.; Böttcher, D.; Matysik, J.; Bornscheuer, U.T.; Zimmermann, W. Conformational Fitting of a Flexible Oligomeric Substrate Does Not Explain the Enzymatic PET Degradation. *Nat. Commun.* **2019**, *10*, 2–6. [CrossRef] [PubMed]
100. Falkenstein, P.; Wei, R.; Matysik, J.; Song, C. Mechanistic Investigation of Enzymatic Degradation of Polyethylene Terephthalate by Nuclear Magnetic Resonance. *Methods Enzymol.* **2021**, *648*, 231–252. [CrossRef] [PubMed]
101. Callaway, E. "The Entire Protein Universe": AI Predicts Shape of Nearly Every Known Protein. *Nature* **2022**, *608*, 15–16. [CrossRef]
102. Hekkelman, M.L.; de Vries, I.; Joosten, R.P.; Perrakis, A. AlphaFill: Enriching AlphaFold Models with Ligands and Cofactors. *Nat. Methods* **2022**, *20*, 205–213. [CrossRef]
103. Furukawa, M.; Kawakami, N.; Tomizawa, A.; Miyamoto, K. Efficient Degradation of Poly(Ethylene Terephthalate) with *Thermobifida fusca* Cutinase Exhibiting Improved Catalytic Activity Generated Using Mutagenesis and Additive-Based Approaches. *Sci. Rep.* **2019**, *9*, 16038. [CrossRef]
104. Herrero Acero, E.; Ribitsch, D.; Dellacher, A.; Zitzenbacher, S.; Marold, A.; Steinkellner, G.; Gruber, K.; Schwab, H.; Guebitz, G.M. Surface Engineering of a Cutinase from *Thermobifida cellulosilytica* for Improved Polyester Hydrolysis. *Biotechnol. Bioeng.* **2013**, *110*, 2581–2590. [CrossRef] [PubMed]
105. Son, H.F.; Cho, I.J.; Joo, S.; Seo, H.; Sagong, H.Y.; Choi, S.Y.; Lee, S.Y.; Kim, K.J. Rational Protein Engineering of Thermo-Stable PETase from *Ideonella sakaiensis* for Highly Efficient PET Degradation. *ACS Catal.* **2019**, *9*, 3519–3526. [CrossRef]
106. Knott, B.C.; Erickson, E.; Allen, M.D.; Gado, J.E.; Graham, R.; Kearns, F.L.; Pardo, I.; Topuzlu, E.; Anderson, J.J.; Austin, H.P.; et al. Characterization and Engineering of a Two-Enzyme System for Plastics Depolymerization. *Proc. Natl. Acad. Sci. USA* **2020**, *117*, 25476–25485. [CrossRef]
107. Wallerstein, J.; Ekberg, V.; Ignjatović, M.M.; Kumar, R.; Caldararu, O.; Peterson, K.; Wernersson, S.; Brath, U.; Leffler, H.; Oksanen, E.; et al. Entropy–Entropy Compensation between the Protein, Ligand, and Solvent Degrees of Freedom Fine-Tunes Affinity in Ligand Binding to Galectin-3C. *JACS Au* **2021**, *1*, 484–500. [CrossRef] [PubMed]
108. Rogers, B.A.; Okur, H.I.; Yan, C.; Yang, T.; Heyda, J.; Cremer, P.S. Weakly Hydrated Anions Bind to Polymers but Not Monomers in Aqueous Solutions. *Nat. Chem.* **2022**, *14*, 40–45. [CrossRef] [PubMed]
109. Chen, X.-Q.; Guo, Z.-Y.; Wang, L.; Yan, Z.-F.; Jin, C.-X.; Huang, Q.-S.; Kong, D.-M.; Rao, D.-M.; Wu, J. Directional-Path Modification Strategy Enhances PET Hydrolase Catalysis of Plastic Degradation. *J. Hazard. Mater.* **2022**, *433*, 128816. [CrossRef]
110. Brizendine, R.K.; Erickson, E.; Haugen, S.J.; Ramirez, K.J.; Miscall, J.; Salvachúa, D.; Pickford, A.R.; Sobkowicz, M.J.; Mcgeehan, J.E.; Beckham, G.T. Particle Size Reduction of Poly(Ethylene Terephthalate) Increases the Rate of Enzymatic Depolymerization But Does Not Increase the Overall Conversion Extent. *ACS Sustain. Chem. Eng.* **2022**, *10*, 9131–9140. [CrossRef]
111. Erickson, E.; Gado, J.E.; Avilán, L.; Bratti, F.; Brizendine, R.K.; Cox, P.A.; Gill, R.; Graham, R.; Kim, D.-J.; König, G.; et al. Sourcing Thermotolerant Poly(Ethylene Terephthalate) Hydrolase Scaffolds from Natural Diversity. *Nat. Commun.* **2022**, *13*, 7850. [CrossRef]
112. Sulaiman, S.; You, D.-J.; Kanaya, E.; Koga, Y.; Kanaya, S. Crystal Structure and Thermodynamic and Kinetic Stability of Metagenome-Derived LC-Cutinase. *Biochemistry* **2014**, *53*, 1858–1869. [CrossRef]
113. Graham, R.; Erickson, E.; Brizendine, R.K.; Salvachúa, D.; Michener, W.E.; Li, Y.; Tan, Z.; Beckham, G.T.; McGeehan, J.E.; Pickford, A.R. The Role of Binding Modules in Enzymatic Poly(Ethylene Terephthalate) Hydrolysis at High-Solids Loadings. *Chem Catal.* **2022**, *2*, 2644–2657. [CrossRef]
114. De Castro, A.M.; Carniel, A.; Nicomedes, J., Jr.; da Conceição Gomes, A.; Valoni, É. Screening of Commercial Enzymes for Poly(Ethylene Terephthalate) (PET) Hydrolysis and Synergy Studies on Different Substrate Sources. *J. Ind. Microbiol. Biotechnol.* **2017**, *44*, 835–844. [CrossRef] [PubMed]

115. Liu, M.; Yang, S.; Long, L.; Cao, Y.; Ding, S. Engineering a Chimeric Lipase-Cutinase (Lip-Cut) for Efficient Enzymatic Deinking of Waste Paper. *BioResources* **2018**, *13*, 981–996. [CrossRef]
116. Liu, M.; Zhang, T.; Long, L.; Zhang, R.; Ding, S. Efficient Enzymatic Degradation of Poly (ε-Caprolactone) by an Engineered Bifunctional Lipase-Cutinase. *Polym. Degrad. Stab.* **2019**, *160*, 120–125. [CrossRef]
117. Ribitsch, D.; Yebra, A.O.; Zitzenbacher, S.; Wu, J.; Nowitsch, S.; Steinkellner, G.; Greimel, K.; Doliska, A.; Oberdorfer, G.; Gruber, C.C.; et al. Fusion of Binding Domains to *Thermobifida cellulosilytica* Cutinase to Tune Sorption Characteristics and Enhancing PET Hydrolysis. *Biomacromolecules* **2013**, *14*, 1769–1776. [CrossRef] [PubMed]
118. Weber, J.; Petrović, D.; Strodel, B.; Smits, S.H.J.; Kolkenbrock, S.; Leggewie, C.; Jaeger, K.E. Interaction of Carbohydrate-Binding Modules with Poly(Ethylene Terephthalate). *Appl. Microbiol. Biotechnol.* **2019**, *103*, 4801–4812. [CrossRef]
119. Xue, R.; Chen, Y.; Rong, H.; Wei, R.; Cui, Z.; Zhou, J.; Dong, W.; Jiang, M. Fusion of Chitin-Binding Domain From *Chitinolyticbacter meiyuanensis* SYBC-H1 to the Leaf-Branch Compost Cutinase for Enhanced PET Hydrolysis. *Front. Bioeng. Biotechnol.* **2021**, *9*, 1315. [CrossRef]
120. Palm, G.J.; Reisky, L.; Böttcher, D.; Müller, H.; Michels, E.A.P.; Walczak, M.C.; Berndt, L.; Weiss, M.S.; Bornscheuer, U.T.; Weber, G. Structure of the Plastic-Degrading *Ideonella sakaiensis* MHETase Bound to a Substrate. *Nat. Commun.* **2019**, *10*, 1717. [CrossRef]
121. Von Haugwitz, G.; Han, X.; Pfaff, L.; Li, Q.; Wei, H.; Gao, J.; Methling, K.; Ao, Y.; Brack, Y.; Mican, J.; et al. Structural Insights into (Tere)Phthalate-Ester Hydrolysis by a Carboxylesterase and Its Role in Promoting PET Depolymerization. *ACS Catal.* **2022**, *12*, 15259–15270. [CrossRef]
122. Puspitasari, N.; Tsai, S.L.; Lee, C.K. Fungal Hydrophobin RolA Enhanced PETase Hydrolysis of Polyethylene Terephthalate. *Appl. Biochem. Biotechnol.* **2021**, *193*, 1284–1295. [CrossRef]
123. Chaires, J.B. Calorimetry and Thermodynamics in Drug Design. *Annu. Rev. Biophys.* **2008**, *37*, 135–151. [CrossRef] [PubMed]
124. Velazquez-Campoy, A.; Markova, N. Isothermal Titration Calorimetry: Theory and Practice. 2015. Available online: https://www.malvernpanalytical.com/en/learn/knowledge-center/whitepapers/wp150318itctheoryandpractice (accessed on 2 November 2022).
125. Tafoukt, D.; Soric, A.; Sigoillot, J.-C.; Ferrasse, J.-H. Determination of Kinetics and Heat of Hydrolysis for Non-Homogenous Substrate by Isothermal Calorimetry. *Bioprocess Biosyst. Eng.* **2017**, *40*, 643–650. [CrossRef] [PubMed]
126. Chan, K.-L.; Ko, C.-H.; Chang, K.-L.; Leu, S.-Y. Construction of a Structural Enzyme Adsorption/Kinetics Model to Elucidate Additives Associated Lignin–Cellulase Interactions in Complex Bioconversion System. *Biotechnol. Bioeng.* **2021**, *118*, 4065–4075. [CrossRef]
127. Thomsen, T.B.; Hunt, C.J.; Meyer, A.S. Standardized Method for Controlled Modification of Poly (Ethylene Terephthalate) (PET) Crystallinity for Assaying PET Degrading Enzymes. *MethodsX* **2022**, *9*, 101815. [CrossRef] [PubMed]
128. Badia, J.D.; Strömberg, E.; Karlsson, S.; Ribes-Greus, A. The Role of Crystalline, Mobile Amorphous and Rigid Amorphous Fractions in the Performance of Recycled Poly (Ethylene Terephthalate) (PET). *Polym. Degrad. Stab.* **2012**, *97*, 98–107. [CrossRef]
129. Carniel, A.; Valoni, É.; Junior, J.N.; da Conceição Gomes, A.; de Castro, A.M. Lipase from *Candida antarctica* (CALB) and Cutinase from *Humicola insolens* Act Synergistically for PET Hydrolysis to Terephthalic Acid. *Process Biochem.* **2017**, *59*, 84–90. [CrossRef]
130. Pellis, A.; Gamerith, C.; Ghazaryan, G.; Ortner, A.; Herrero Acero, E.; Guebitz, G.M. Ultrasound-Enhanced Enzymatic Hydrolysis of Poly(Ethylene Terephthalate). *Bioresour. Technol.* **2016**, *218*, 1298–1302. [CrossRef]
131. Morshed, M.N.; Bouazizi, N.; Behary, N.; Guan, J.; Nierstrasz, V. Stabilization of Zero Valent Iron (Fe0) on Plasma/Dendrimer Functionalized Polyester Fabrics for Fenton-like Removal of Hazardous Water Pollutants. *Chem. Eng. J.* **2019**, *374*, 658–673. [CrossRef]
132. Farhadi, A.R.K.; Rahemi, N.; Allahyari, S.; Tasbihi, M. Metal-Doped Perovskite BiFeO3/RGO Nanocomposites towards the Degradation of Acetaminophen in Aqueous Phase Using Plasma-Photocatalytic Hybrid Technology. *J. Taiwan Inst. Chem. Eng.* **2021**, *120*, 77–92. [CrossRef]
133. Schmidt, J.; Wei, R.; Oeser, T.; Belisário-Ferrari, M.R.; Barth, M.; Then, J.; Zimmermann, W. Effect of Tris, MOPS, and Phosphate Buffers on the Hydrolysis of Polyethylene Terephthalate Films by Polyester Hydrolases. *FEBS Open Bio* **2016**, *6*, 919–927. [CrossRef]
134. Barth, M.; Wei, R.; Oeser, T.; Then, J.; Schmidt, J.; Wohlgemuth, F.; Zimmermann, W. Enzymatic Hydrolysis of Polyethylene Terephthalate Films in an Ultrafiltration Membrane Reactor. *J. Memb. Sci.* **2015**, *494*, 182–187. [CrossRef]
135. Carniel, A.; Gomes, A.D.C.; Coelho, M.A.Z.; de Castro, A.M. Process Strategies to Improve Biocatalytic Depolymerization of Post-Consumer PET Packages in Bioreactors, and Investigation on Consumables Cost Reduction. *Bioprocess Biosyst. Eng.* **2021**, *44*, 507–516. [CrossRef] [PubMed]
136. De Queiros Eugenio, E.; Campisano, I.S.P.; de Castro, A.M.; Coelho, M.A.Z.; Langone, M.A.P. Experimental and Mathematical Modeling Approaches for Biocatalytic Post-Consumer Poly(Ethylene Terephthalate) Hydrolysis. *J. Biotechnol.* **2021**, *341*, 76–85. [CrossRef] [PubMed]
137. CARBIOS Investor Day 2022 Presentation. 2022. Available online: https://www.carbios.com/en/regulated-information/page/2/ (accessed on 2 March 2023).
138. Singh, A.; Rorrer, N.A.; Nicholson, S.R.; Erickson, E.; DesVeaux, J.S.; Avelino, A.F.T.; Lamers, P.; Bhatt, A.; Zhang, Y.; Avery, G.; et al. Techno-Economic, Life-Cycle, and Socioeconomic Impact Analysis of Enzymatic Recycling of Poly(Ethylene Terephthalate). *Joule* **2021**, *5*, 2479–2503. [CrossRef]

139. Kawai, F. Emerging Strategies in Polyethylene Terephthalate Hydrolase Research for Biorecycling. *ChemSusChem* **2021**, *14*, 4115–4122. [CrossRef]
140. Kawai, F. The Current State of Research on PET Hydrolyzing Enzymes Available for Biorecycling. *Catalysts* **2021**, *11*, 206. [CrossRef]
141. Anishchenko, I.; Pellock, S.J.; Chidyausiku, T.M.; Ramelot, T.A.; Ovchinnikov, S.; Hao, J.; Bafna, K.; Norn, C.; Kang, A.; Bera, A.K.; et al. De Novo Protein Design by Deep Network Hallucination. *Nature* **2021**, *600*, 547–552. [CrossRef]
142. Jumper, J.; Evans, R.; Pritzel, A.; Green, T.; Figurnov, M.; Ronneberger, O.; Tunyasuvunakool, K.; Bates, R.; Žídek, A.; Potapenko, A.; et al. Highly Accurate Protein Structure Prediction with AlphaFold. *Nature* **2021**, *596*, 583–589. [CrossRef] [PubMed]
143. Wang, J.; Lisanza, S.; Juergens, D.; Tischer, D.; Watson, J.L.; Castro, K.M.; Ragotte, R.; Saragovi, A.; Milles, L.F.; Baek, M.; et al. Scaffolding Protein Functional Sites Using Deep Learning. *Science* **2022**, *377*, 387–394. [CrossRef]
144. Dauparas, J.; Anishchenko, I.; Bennett, N.; Bai, H.; Ragotte, R.J.; Milles, L.F.; Wicky, B.I.M.; Courbet, A.; de Haas, R.J.; Bethel, N.; et al. Robust Deep Learning–Based Protein Sequence Design Using ProteinMPNN. *Science* **2022**, *378*, 49–56. [CrossRef]
145. Ferruz, N.; Heinzinger, M.; Akdel, M.; Goncearenco, A.; Naef, L.; Dallago, C. From Sequence to Function through Structure: Deep Learning for Protein Design. *bioRxiv* **2022**, *21*, 238–250. [CrossRef] [PubMed]
146. Wicky, B.I.M.; Milles, L.F.; Courbet, A.; Ragotte, R.J.; Dauparas, J.; Kinfu, E.; Tipps, S.; Kibler, R.D.; Baek, M.; DiMaio, F.; et al. Hallucinating Symmetric Protein Assemblies. *Science* **2022**, *378*, 56–61. [CrossRef] [PubMed]

Disclaimer/Publisher's Note: The statements, opinions and data contained in all publications are solely those of the individual author(s) and contributor(s) and not of MDPI and/or the editor(s). MDPI and/or the editor(s) disclaim responsibility for any injury to people or property resulting from any ideas, methods, instructions or products referred to in the content.